Sources and processes that control the submicron organic aerosol in an urban Mediterranean environment (Athens) using high temporal resolution chemical composition measurements.

Iasonas Stavroulas[1,2,3], Aikaterini Bougiatioti[1,3], Georgios Grivas[3], Despina Paraskevopoulou[3], Maria Tsagkaraki[1], Pavlos Zarmpas[1], Eleni Liakakou[3], Evangelos Gerasopoulos[3] and Nikolaos Mihalopoulos[1,3]

[1]Environmental Chemical Processes Laboratory, Department of Chemistry, University of Crete, 71003 Crete, Greece
[2]Energy Environment and Water Research Center, The Cyprus Institute, Nicosia 2121, Cyprus
[3]Institute for Environmental Research and Sustainable Development, National Observatory of Athens, Lofos Koufou, P. Penteli, 15236, Athens, Greece

Correspondence to: A. Bougiatioti (kbougiatioti@gmail.com) and N. Mihalopoulos (nmihalo@noa.gr)

Abstract. Submicron aerosol chemical composition has been studied during a year-long period (26/07/2016-31/07/2017) and two winter-time intensive campaigns (18/12/2013 – 21/02/2014 and 23/12/2015 – 17/02/2016), at a central site in Athens, Greece, using an Aerosol Chemical Speciation Monitor (ACSM). Concurrent measurements include a Particle-Into-Liquid Sampler (PILS-IC), a Scanning Mobility Particle Sizer (SMPS), an AE-33 Aethalometer and Ion Chromatography analysis on 24 or 12 hour filter samples. The aim of the study was to characterize the seasonal variability of the main submicron aerosol constituents and decipher the sources of organic aerosol (OA). Organics were found to contribute almost half of the submicron mass, with 30-min resolution concentrations during wintertime reaching up to 200 μg m^{-3}. During winter (all three campaigns combined), the primary sources contribute about 33% of the organic fraction, comprising of biomass burning (10%), fossil fuel combustion (13%) and cooking (10%), while the remaining 67% is attributed to secondary aerosol. The semi-volatile component of the oxidized organic aerosol (SV-OOA; 21.8%) was found to be clearly linked to combustion sources and in particular biomass burning, and even a part of the very oxidized, low-volatility component (LV-OOA; 44%) could also be attributed to the oxidation of emissions from these primary combustion

sources. These results, based on the combined contribution of BBOA and SV-OOA, highlight the rising importance of biomass burning in urban environments during wintertime, as revealed through this characteristic example of Athens, Greece, where the economic recessions led to an abrupt shift to biomass burning for heating purposes in winter. During summer, when concentrations of fine aerosols are considerably lower, more than 80% of the organic fraction is attributed to secondary aerosol (SV-OOA 31% and LV-OOA 53%). In contrast to winter, SV-OOA appears to result from a well-mixed type of aerosol, linked to fast photochemical processes and the oxidation of primary traffic and biogenic emissions. Finally, LV-OOA presents a more regional character in summer, owing to the oxidation, within a few days, of organic aerosol.

1. Introduction (This sections has been rewritten)

Exposure to fine particulate matter is recognized as a leading cause of premature mortality in Europe. Even if the annual limit value is not exceeded at the majority of regulatory monitoring stations in European countries, health effects are expected to appear at lower levels as well, even below the WHO guideline values (EEA, 2017).

Organic carbon (OC) is among the key PM components which record the strongest associations with short-term mortality (Ito et al., 2011; Klemm et al., 2011). Moreover, short-term exposure to OC has also been linked to respiratory and cardiovascular hospital admissions (Levy et al., 2012; Zanobetti et al., 2009) and pediatric asthma ED visits (Strickland et al., 2010).

It appears that the characterization of fine aerosol chemical properties and their short term variability is critical, especially at the urban background level which is more relevant for the average population exposure. While the majority of transformations related to particle sulfate and nitrate have been well described, there is much progress to be made regarding the mechanisms and characteristics of secondary organic products.

The development of the Aerosol Mass Spectrometer (AMS) technology has been an important breakthrough in the study of aerosol chemical composition, in high temporal resolution. The ability to further differentiate between primary and secondary components, based on specific markers, introduces an important advancement to organic aerosol (OA) source apportionment (Jimenez et al., 2009), which otherwise mainly relied on a statistical approach using elemental and organic carbon thermal-optical data (EC tracer method and variants; Turpin and Huntzicker, 1995). Capitalizing on abundant spectroscopic data, PMF (Positive Matrix Factorization) source

apportionment (SA) is used to discern between various primary sources like traffic and biomass burning, and to categorize secondary aerosols depending on their degree of oxidation.

The ACSM (Aerosol Chemical Speciation Monitor) is an instrument relying on AMS technology and is specifically designed for long-term routine monitoring (Ng et al., 2011). While many studies have focused at regional and rural background areas, ACSM results from large European urban centers are relatively scarce. Canonaco et al. (2013) have performed one year of measurements at an urban background site in the center of Zurich. Aurela et al. (2015) have deployed an ACSM at residential, traffic and highway sites within the Metropolitan Area of Helsinki, for a total of five months. Findings from 10 months of measurements at the North Kensington urban background site in London are reported by Reyes-Villegas et al. (2016).

Regarding Southern European cities, results have been presented from the intensive ACSM campaign of Minguillon et al. (2016), at an urban background site in Barcelona. Short-term – up to one month - studies in Southern Europe using the AMS have also been conducted in Barcelona (Mohr et al., 2012), Bologna (Gilardoni et al., 2016) and Marseille (El Haddad et al., 2013). In urban Athens, a one-month AMS campaign during winter 2013 has been carried out for chemical composition and OA sources (Florou et al., 2017).

The Greater Athens Area (GAA) appears as a challenging urban milieu for the study of aerosol dynamics, as it combines a large population (about 4 million) and intense primary emissions, with complex topography and meteorology, that lead to high levels of atmospheric pollutants and significantly deteriorate air quality (Kanakidou et al., 2011; Pateraki et al., 2014). The characteristics and related processes of secondary organic aerosols, in the long-term, have received up to this point limited attention (Grivas et al., 2012; Paraskevopoulou et al., 2014).

Moreover, since 2013, due to the economic recession in Greece, primary and secondary precursor emissions emerge altered and intensified, as the residents have switched from fossil fuel combustion to uncontrolled burning of wood and biomass for space heating (Saffari et al., 2013, Fourtziou et al., 2017, Gratsea et al., 2017). Existing measurements of aerosol chemical composition in Athens have mainly been performed using filter sampling (Theodosi et al., 2011, 2018; Paraskevopoulou et al., 2014) and have indicated the dominant role of organic aerosols in the fine particle fraction.

In this study we present, for the first time, long-term results on the sources of submicron organic aerosols in Athens from high temporal resolution measurements during a year-long period,

complemented by two intensive winter campaigns. For the collection of data, we deployed an Aerosol Chemical Speciation Monitor (ACSM) and in addition a Particle Into Liquid Sampler (PILS) coupled with ion chromatography, an AE-33 Aethalometer, while also conducting auxiliary aerosol (filter-based) and gas phase measurements.

The main objectives of this are (i) to characterize the submicron aerosol and its variability using high temporal resolution, (ii) to quantify the sources of the organic aerosol and their seasonal variability (via PMF analysis) and (iii) to study the year-to-year changes of aerosol sources during winter time, with special emphasis on wood burning.

2. Experimental Methods

2.1 Sampling site and period

The measurements exploited in this study were conducted, at the urban background site of the National Observatory of Athens at Thissio (37.97N, 23.72E), as representative of the mean population exposure over Athens metropolitan area (Fourtziou et al., 2017). The site stands at an elevation of 105 m above sea level, in a moderately populated area, where the influence of direct local emissions is limited.

The measurement period lasted for an entire year, from July 2016 to July 2017. Additionally, two intensive winter campaigns took place at the same site, the first from mid-December 2013 to mid-February 2014 and the second from 23 December 2015 to 17 February 2016. These intensive campaigns aimed at studying the year-to-year variability and impact of biomass burning on the air quality of the city of Athens during wintertime.

2.2 Instruments and Methods

Measurements were performed with an Aerosol Chemical Speciation Monitor (ACSM) by Aerodyne Research Inc. (Ng et al. 2011a), measuring the non-refractory PM_1 (NR-PM_1) chemical composition in near real-time (30-minute temporal resolution). The instrument was sampling through a BGI Inc. SCC 1.197 Sharp Cut Cyclone operated at 3 L min^{-1}, yielding a cut off diameter of approximately 2 μm. Practically the ACSM operates following a similar principle as the Aerosol Mass Spectrometer (AMS) (Jayne et al., 2000) where ambient air is drawn through a critical orifice to a particle focusing aerodynamic lens; the resulting particle beam is flash-vaporized at 600°C, ionized via electron impact ionization and guided through a quadrupole mass

spectrometer. Ammonium nitrate and ammonium sulfate calibrations were performed prior to the ACSM's deployment on the site for the period of 2016 – 2017 and the response factor (RF) for nitrate along to the Relative Ionization Efficiencies (RIEs) for ammonium and sulfate were determined. For the 2013 – 2014 and 2015 – 2016 intensive winter campaigns ammonium nitrate calibration were performed and the RIE for sulfate was determined according to the fitting approach proposed by Budisulistiorini et al. (2014). Values are presented in Table ST1 of the supplementary material. The detection limits for the ACSM provided by Ng et al. (2011a) are: 0.284 μg m^{-3} for ammonium, 0.148 μg m^{-3} for organics, 0.024 μg m^{-3} for sulfate, 0.012 μg m^{-3} for nitrate, and 0.011 μg m^{-3} for chloride. Mass concentrations are calculated using a chemical composition dependent collection efficiency (Middlebrook et al., 2012) (Fig. SF.1).

Parallel measurements were performed for biomass burning identification, but also for quality control purposes. In this context, a Metrohm ADI 2081 Particle Into Liquid Sampler (Orsini et al., 2003) coupled with Ion Chromatography (Dionex ICS-1500) was used, which was sampling ambient air from a different, but adjacent to the ACSM's, PM_1 inlet. Two denuders were placed inline, upstream of the instrument in order to remove gas phase species (e.g. NH_3, HNO_3, SO_2) The ion Chromatograph was set to measure cations such as ammonium and potassium at a time resolution of 15 minutes. The resulting concentrations from the ACSM were tested against filter measurements and the concentrations provided by the PILS. For the PILS, the detection limit was calculated at 1 ppb for Na^+, NH_4^+ and 2 ppb for K^+. nss-K^+ concentrations were calculated using the Na^+ concentrations and the Na^+/K^+ ratio in seawater as a reference (Sciare et al., 2005). Reported concentrations were blank corrected.

Furthermore, filter sampling was also conducted in parallel at the Thissio station. $PM_{2.5}$ aerosol samples on Quartz fiber filters (Flex Tissuquartz, 2500QAT-UP 47mm, PALL) were collected on a daily basis while during the winter periods the sampling frequency was set to 12h. A Dichotomous Partisol Sampler 2025 (Ruprecht & Patashnick) was used at a flow rate of 16.7 L min^{-1}. The samples were analyzed for organic and elemental carbon (OC, EC) with the Thermal-Optical Transmission technique, using a Sunset Laboratories OC/EC Analyzer and applying the EUSAAR-2 protocol (Cavalli et al., 2010). Filters where also analyzed for determination of the main ionic species using ion chromatography as described in Paraskevopoulou et al. (2014).

Two different absorption photometers were monitoring Black Carbon (BC) concentrations. A 7-wavelength Magee Scientific AE-42 portable aethalometer was used for the 2013-14 and 2015-

155   16 winter campaigns, providing 5-min resolution measurements. For the year-long period a dual
      spot, 7-wavelength Magee Scientific AE-33 aethalometer (Drinovec et al., 2015) was used,
      operating at 1-min resolution. Standard gas analyzers for O_3 (Thermo Electron Co., model: 49i),
      CO, SO_2 and NO_x (HORIBA, 360 series) and a Scanning Mobility Particle Sizer for PM_1 size
      distributions (SMPS 3034, TSI Inc.) measuring in the range of 10.4 – 469.8 nm, were also
160   operating at the sampling site. Wavelength dependent source apportionment of the BC load was
      performed by the AE-33 Aethalometer, based on the approach of Sandradewi et al. (2008)
      providing a fossil fuel (BC_{ff}) and a wood combustion (BC_{wb}) component. The default absorption
      exponents of 1 for fossil fuel combustion and 2 for pure wood burning, as incorporated in the AE-
      33 software, was used, very close to the respective values of 0.9 and 2, used in a suburban site in
165   Athens (Kalogridis et al., 2017). Meteorological parameters for the study were taken from the
      actinometric meteorological station of NOA, at Thissio (Kazadzis et al., 2018) (Fig. SF.2). All
      measurements were averaged to 1-hour intervals in order to synchronize the different data sets.

      The bivariate wind speed-direction plotting methodology developed by Carslaw and Ropkins
      (2012) in the Openair R-package, was used for the identification of source areas, as incorporated
170   in the Zefir Igor Pro-based tool (Petit et al., 2017). Four-day back trajectories were calculated using
      the HYbrid Single-Particle Langrangian Integrated Trajectory (HYSPLIT_4) model (Draxler and
      Hess, 1998) developed by the ARL/NOAA, and 1-degree GDAS (NCEP) meteorological data.
      Trajectories were computed every 3-h, for air masses arriving at Athens at a height of 1000 m. The
      selected height is considered suitable to capt ure transport at a representative upper limit of the
175   boundary layer in Athens (Markou and Kassomenos, 2010). Trajectory clustering was performed
      using the TrajStat plugin (Sirois and Bottenheim, 1995; Wang et al., 2009) of the MeteoInfo GIS
      software. The change of the total space variance for decreasing number of clusters was examined
      as a criterion for cluster number selection. The analysis was performed separately for summer and
      winter, resulting in 5 clusters for each period.

180

2.3 Source apportionment of the submicron organic fraction using PMF analysis.

2.3.1 PMF strategy.

Positive Matrix Factorization (Paatero and Tapper, 1994) was performed on the organic mass
spectra obtained by the ACSM. The graphic interface SoFi (Source Finder) version 6.1, developed
185   at PSI, Zurich (Canonaco et al., 2013) was used. SoFi implements the multilinear engine algorithm

ME-2 (Paatero and Hopke, 2003), analyzing the acquired mass spectral timeseries matrix into a linear combination of factor profile (FP) and time series sub-matrices. Detailed description of the method can be found in the above referenced studies.

For our datasets only m/z ≤ 125 were used in order to avoid interferences from the naphthalene signal (m/z 127, 128 and 129). Weak signals, with signal-to-noise ratio (S/N) below 0.2 were downweighted by a factor of 10, and those with S/N between 0.2 and 1 were downweighted by a factor of 2 (Ulbrich et al., 2009), using built in utilities of the SoFi toolkit.

The input organics and organics' error matrices are derived automatically from the ACSM data analysis software. Several model runs were performed, with and without applying constrains to the derived FPs, using the α value approach (Canonaco et al., 2013; 2015) and following the methodology proposed by Crippa et al. (2014). Initially unconstrained PMF runs provided insight on the potential number and type of factors. For the following steps, reference factor profiles (RFPs) were introduced in order to constrain primary OA factors, (i) first for the Hydrocarbon – like organic aerosol (HOA), (ii) then for both HOA and BBOA and (iii) finally for HOA, BBOA plus cooking – like organic aerosol (COA). Potential FPs for secondary organic aerosols were left unconstrained. A thorough discussion on the choice and representativeness of the RFPs used can be found in section SI.4.1 of the supplementary material. Each factor was constrained using different α values within the limits suggested by Crippa et al. (2014). Next, the model's residuals, for each different model setup, were analyzed in search of structures that could indicate underestimation or overestimation of the number of separated factors. Stability of factors for different model seeds and correlations of the obtained FP spectra with FPs reported in similar environments and conditions were examined (Section SI.4.8). Finally, correlations of the time series of the selected optimal solutions to both gas phase and particulate independent measurements such as BC, BC_{ff}, BC_{wb}, CO, nss-K^+, NO_3^-, $SO_4^{2=}$ and NH_4^+ was examined to solidify the selection (Section SI.4.9).

The year-long data series was divided into a cold period, from November 2016 to March 2017 and warm period consisting of two sub-periods from August to September 2016 and from May to July 2017 which were treated separately. According to studies on the climatology of Southern Greece, the transient period (spring and fall seasons) in Athens doesn't exceed 60 days on average (Argyriou et al., 2004), covering mainly the months of April and October - which were excluded

from the seasonal analysis (Figure SF.1). The two wintertime campaigns of 2013-2014 and 2015-2016 were also treated separately.

The coefficient of determination r^2 for simple linear regression is used as a metric for all comparisons, e.g. both affinity of obtained FPs with literature spectra and correlation of the respective time series with independent measurements.

2.3.2 Choosing the optimal configuration

Presentation of, and discussion on the optimal configuration chosen for the ME-2 model, as well as results from each step of the implemented strategy described above, followed by a sensitivity analysis on the α value influence on the obtained factors, can be found in section SI.4. In brief, for the cold period and the two winter – time intensive campaigns, constraining three factors, namely HOA, BBOA and COA, and leaving two unconstrained SOA factors, produces a solution that is characterized by minimal seed variability and model residual structures, while FPs, time-series, relative contribution and diurnal variability of the factors appear to be environmentally relevant, resembling solutions proposed earlier for the region (Kostenidou et al., 2015; Florou et al., 2017). Leaving factors unconstrained leads to an unstable model behavior such as diurnal residual structures for key variables (e.g. alkyl fragments like m/z=55 or 57) and large FP variability for different model seed runs. Furthermore, deconvolved spectra were missing expected variable contributions in profiles such as BBOA (very low m/z=41 and 43 relative contributions), while the COA – like factor was dominated by the CO_2^+ fragment at m/z=44. Configuring less or more than five factor solutions, resulted either in an even more pronounced residual diurnal cycle, pointing to poor factor separation or in splitting behavior and resulting factors which were environmentally irrelevant.

On the other hand, for the warm period constraining two factors, namely HOA and COA, and leaving two unconstrained SOA factors was found to be the solution exhibiting higher relevance while being robust and close to previous knowledge related to OA in the Greater Athens Area. A BBOA factor could not be identified for the warm periods, since contribution of the marker fragments for biomass burning m/z=60 and m/z=73 are almost absent in these periods dataset. The COA factor is present in all the studied periods, validated following the approach of Mohr et al.

(2012) (Fig. SF.9), and emerged in all the steps (unconstrained and constrained runs) of the implemented strategy (Figures SI.4 through SI.7 and related discussion in section SI.4).

3. Results and Discussion

3.1 Comparison of ACSM data with ancillary measurements

As a first quality control/quality assurance of the ACSM data, the ammonium concentrations are compared to the respective ones derived from the PILS, on an hourly basis for winter 2016-17. A good agreement is found (r^2=0.80, slope of 0.82). The sulfate and nitrate concentrations for the winter 2016-2017 period are compared to the respective ones from the ion chromatography analysis ($PM_{2.5}$ filters), on a daily basis (r^2=0.75, slope of 0.81 and r^2=0.78, slope of 0.95, respectively). The organics concentrations are compared to the organic carbon concentrations of the $PM_{2.5}$ filters. An excellent agreement is found (r^2=0.93, slope of 1.59) with the slope being close to values reported for urban areas (Petit et al., 2015) and OM:OC calculations from AMS measurements in polluted environments (Saarikoski et al., 2012). The results from the aforementioned comparisons are provided in the Supplementary material (SF.3).

During the intensive winter 2015-2016 campaign, the concentrations of the ACSM components are compared to those determined from the ion chromatography, based on concurrent filter samples collected at the same site, twice per day, (06:00 - 18:00 pm and t 18:00 - 06:00 local time). Results indicate an excellent agreement for sulfate (r^2=0.88, slope of 1.0), ammonium (r^2=0.82, slope of 1.06), and nitrate (r^2=0.88, slope of 1.12) (Figure SF.4). During the intensive winter 2013-2014 campaign, the ammonium concentrations from the ACSM showed significant correlation with the respective ones from the PILS (r^2=0.80, slope of 0.81).

Finally, the sum of the ACSM component concentrations plus BC, measured with the 7-wavelength aethalometer was compared with the mass concentrations determined by the SMPS since February 2017 at Thissio. The density used to convert volume distributions and consequently volume concentrations of spherical particles to mass concentrations, was obtained by applying the methodology of Bougiatioti et al. (2014) assuming that the aerosol PM_1 population was dominated by ammonium sulfate and organics and calculating the respective mass fractions time series based on the ACSM measurements. A density of 1.77 g cm^{-3} was used for ammonium sulfate and 1.3 g cm^{-3} for organics (Florou et al., 2017). The results obtained using a chemical dependent collection

efficiency to determine the ACSM derived mass concentrations, are portrayed in Figure 1 and indicate excellent correlation (r^2=0.89) a slope of 0.96 and an intercept of 0.60.

3.2 PM$_1$ average chemical composition and temporal variability

3.2.1 Chemical composition and characteristics

The time series of the main submicron aerosol components measured by the ACSM and the black carbon concentrations are presented in the upper panel of Figure 2 (one complete year period). The periods average cumulative concentration of the ACSM components and BC was 12.4±12.5 μg m^{-3}. The highest concentrations were measured during winter (average 16.1±19.5 μg m^{-3}) and the lowest during summer (average 10.3±5.6 μg m^{-3}). On an annual basis, the most abundant component was organic aerosol, followed by sulfate, contributing 44.5 and 27.8% to the total submicron mass, respectively, while BC contribution was calculated at 15.1%, ammonium 7.9% and nitrate 4.3%. In the middle and bottom panels of Figure 2 the respective time series of the main submicron aerosol components during the two intensive 2-month winter campaigns are presented. During winter 2013-14 the average mass concentration of the ACSM components (plus BC concentrations) was 24.5±24.7 μg m^{-3}, with organics and BC contributing 55.6 and 14.6% to the total submicron mass, respectively, followed by sulfate (13.6%). During winter 2015-16 the average concentration was 21.2±27.4 μg m^{-3}, with organics and BC contributing 51.6 and 15.2% to the total submicron mass, respectively, followed by sulfate (14.8%), nitrate (6.5%) and ammonium (6.7%). It is clearly deduced that during the last winters, organics constitute half or even more of the total PM$_1$ mass, sulfate around 20% and BC around 14%.

The other striking feature is that during wintertime, PM$_1$ concentration spikes can reach up to 220 μg m^{-3} hourly values, with organics taking up most of the mass. Maxima are recorded during night-time and mostly during meteorological conditions favoring pollutants emission and accumulation, such as low wind speed and low temperature (Fourtziou et al., 2017). There are on average 8 such incidents occurring during each winter (10 in 2013-14, 7 in 2015-16 and 7 in 2016-17), with organic levels being higher than 100 μg m^{-3}. To our knowledge, such levels are the highest reported for Europe during wintertime and highlight the strong impact of local emissions and especially those related to heating/wood burning (see below), on the levels of organics and consequently PM$_1$. Similar maxima to the ones observed in this study are also reported by Florou et al. (2017, same site from 10 January until 9 February 2013), where organics concentration alone

reached up to 125 μg m^{-3} and maxima of 8 μg m^{-3} for BC and up to 5 μg m^{-3} for nitrate, were recorded. Similarly, wintertime pollution events with increased local character and elevated organics concentrations (around 100 μg m^{-3}, average of 22.6 μg m^{-3}) have been reported at a regional background site, just outside of Paris, during February 2012 (Petit et al., 2015).

3.2.2 Seasonal variability

The seasonal variability of the main measured species, along with the average PM$_1$ concentration (μg m^{-3}), as calculated from the ACSM+BC measurements is shown in Figure 3 and the basic statistics are included in Table 1. Organics contribute 46% to the total submicron aerosol mass in summer, followed by sulfate (30.5%), BC (12.6%), ammonium (8.3%) and nitrate (2.6%) , while in winter, organics and sulfate contribute 48.1 and 23.2%, respectively, followed by BC (14.7%), ammonium (6.9%) and nitrate (6.3%).

The mass concentrations of organics, nitrate, chloride and BC exhibit a clear annual cycle, with minimum during summer and maximum in winter. This pattern seems to be due to a combination of three simultaneous processes. At first, the additional primary emissions from domestic heating play an important role, as is evident by the largely elevated concentration levels of organics and BC, which during winter are also emitted by central heating systems and fireplaces. A second reason could be the decreased boundary layer depth during winter. According to Kassomenos et al., 1995 and Alexiou et al., 2018, daytime PBL depth shows a clear annual cycle, with maxima during the warm months (June to September) and exhibiting a two-fold decrease during wintertime. Finally, the effect of temperature to the partitioning of the semi-volatile inorganics and organics can also contribute to the processes leading to the observed pattern. In support of the above, larger standard deviation is found in winter, demonstrating the frequency and magnitude of the observed pollution events due to the increased need for heating purposes (Fourtziou et al., 2017). Independently of the year, it can be seen that winter concentrations of organics, nitrate, chloride and BC are very similar and more than twice the respective ones during the rest of the seasons (Table 1).

Organics concentration are consistently high during all studied winters (from December to February), while the higher nitrate values, exhibiting similar trend with organics and BC can be attributed to the combination of lower temperatures during night-time along with the increased combustion sources which lead to reduced acidity, resulting at the favorable partitioning of nitrate

in the aerosol phase. (Park et al., 2005; Mariani and de Mello, 2007; Guo et al., 2016). Ammonium and sulfate exhibit the opposite seasonal cycle, with maximum values in summer and minimum during winter and spring. The higher summer sulfate levels are the result of enhanced photochemistry associated with more intense insolation, combined with less precipitation, favoring the regional transport of polluted air masses (Cusack et al., 2012). The seasonal variation of concentrations is in agreement with that observed in Athens, during prior long-term measurement campaigns based on analysis of daily filter samples (Theodosi et al. 2011, Paraskevopoulou et al., 2014; 2015).

3.2.3 Diurnal variability

When investigating the diurnal patterns of the measured species (Figure 4), it is observed that during wintertime, ammonium and sulfate do not exhibit any significant variability, which is due to the regional character of ammonium sulfate. In order to quantify the extent of this variability we calculated the normalized diurnal pattern by dividing each hourly value with the respective mean concentration. More specifically, sulfate varies by 13% around the mean value while ammonium varies by 40%. On the other hand, organics, BC and nitrate vary significantly during the day (183%, 79.8% and 110% respectively). These species clearly double their concentrations during night-time, caused by the additional primary emissions. Furthermore, BC also exhibits a second maximum during early morning hours, which should be attributed to the primary emissions during the morning traffic rush–hour.

During summer, all concentrations are significantly lower, especially organics (note scale change) which exhibit a 5-fold decrease of their mean maximum concentration during night-time. Normalizing the diurnal cycles, as mentioned above, reveals a much less pronounced variability for organics (65%), implying a more regional character, while BC and nitrate exhibit the highest variability (67.7% and 77% respectively) in accordance to their local nature. The night-time maxima of BC vanishes, while nitrate shows much lower concentrations, due to nitrate partitioning between gas and aerosol phase, favoring the vaporization of ammonium nitrate. BC still exhibits only one maximum during early morning hours owing to traffic emissions. Ammonium and sulfate diurnal profile follows expected photochemistry patterns, with peaking concentrations around 14:00 LT (UTC+2), consistent with secondary aerosol formation and increased vertical mixing with regional aerosol from aloft due to the evolution of the convective boundary layer which

exhibits a bell shaped diurnal structure ranging from a few hundred meters to above one kilometer, with maximum heights during early afternoon (Asimakopoulos et al., 2004; Tombrou et al., 2007). Finally, organics concentrations are somewhat higher during early night which could possibly be associated with biogenic/vegetation sources either local or regional that produce volatile compounds and condense on the particulate phase during night when temperatures are lower, as is further elaborated during the source apportionment results discussion in section 3.3. Furthermore, organic variation also follows the late afternoon peak also observed for ammonium and sulfate. Condensation of the particulate phase could apply for nitrate as well, which also exhibits higher concentrations during night-time (almost double).

3.3 Source apportionment of organic aerosol
.

Warm period: In this period, the selected solution is a two factor constrained run (HOA using α =0.05 and COA using α =0.1) and consists of four factors: HOA, COA-like, SV-OOA (semi-volatile oxygenated OA) and LV-OOA (low-volatility oxygenated OA). As already mentioned, the two summer periods have been treated separately, but the derived spectra were almost identical (r^2 ranging from 0.98-0.99). The time series of the four identified sources during summer 2017 is shown in Figure 5 along with their diurnal variability and the respective average daily contribution. The mass spectra of the selected solution are also provided in the supplementary material (Fig SF.12). No primary biomass burning aerosol could be identified, which is justified by the absence of fresh emissions over the city center during the warm period. In the summer periods HOA makes up 4.3% of the total organic fraction, COA around 10% on average (7.3 and 11.3% for 2016 and 2017, respectively). In summer 2016 SV-OOA made up 32% and the rest 56% is LV-OOA. In summer 2017, SV-OOA contributes 34.6% to the total organic fraction while LV-OOA 49.7%. The dominance of secondary influence (SV-OOA & LV-OOA) is apparent, and accounts for the majority of the organic aerosol. This finding is in accordance with Kostenidou et al. (2015), who reported that 65% of the sampled aerosol during summer can attributed to SOA (SV-OOA & LV-OOA), at a suburban site in Athens.

A comparison of the derived FPs with mass spectra in literature is shown in Fig SF.15-19 in the supplement. COA FP exhibits excellent correlation with spectra obtained in previous studies

in the city (Florou et al., 2017; Kostenidou et al., 2015) as well as with spectra obtained in laboratory experiments investigating fresh OA emissions from meat charbroiling (Kaltsonoudis et al., 2017). When calculating the O:C ratio in COA following the study of Canagaratna et al. (2015) we find a ratio of 0.19, which is comparable to the value of 0.24 obtained for COA during summer at a suburban site in Athens (Kostenidou et al., 2015).

The HOA FP exhibits excellent correlation with literature spectra measured in cities located in the Mediterranean environment (Florou et al., 2017; Kostenidou et al., 2015; Gilardoni et al., 2016) as well as in other environmental and socioeconomical settings (Crippa et al., 2013; Lanz et al., 2009). According to Figure SF.18, where the affinity of SV-OOA with literature spectra is assessed, some assumptions could be made regarding the origin of the factor in this study. Similarity with IEPOX – OA, which is the oxidation product of isoprene, could denote a possible link of SV-OOA with biogenic aerosol. This association is further strengthened by considering the excellent correlation with SOA from biogenic precursors, such as a- and b-pinene reported by Bahreini et al., (2005) (r^2 *of* 0.86 and 0.89, respectively). These precursors are found to exhibit maxima during night-time (Harrison et al., 2001; Li et al., 2018; Hatch et al., 2011) coinciding with the diurnal behavior of SV-OOA in this study. On the other hand, comparison of the derived SV-OOA with SOA from diesel exhaust after 4 h of photochemical ageing (Sage et al. 2008) yields an r^2 *of* 0.89. Finally, SV-OOA exhibits the lowest correlations with the mass spectrum from aged organic aerosol emissions from meat charbroiling (Kaltsonoudis et al., 2017). The above mentioned comparisons with literature FPs provides some indication that during summer, SV-OOA could be linked to SOA formation from the oxidation of VOCs from both biogenic and traffic sources and is not linked to the oxidation of primary COA. The low volatility component derived, exhibits excellent correlation to the very oxidized regional OOA found in the area (Bougiatioti et al., 2014) and good correlation with deconvolved OOA factors from previous studies in Athens (Florou et al., 2017; Kostenidou et al., 2015). When calculating the elemental ratios based on the study of Canagaratna et al. (2015), the O:C ratio for LV-OOA is 1.2, which is identical to the value of OOA obtained at Finokalia (Bougiatioti et al. 2014).

In terms of comparison with independent measurements, HOA exhibits good correlation with nitrate (r^2=0.62) as well as with BC$_{ff}$ (r^2=0.63) while COA, as expected, shows poor correlation with CO (r^2=0.33) and nitrate (r^2=0.36). SV-OOA is highly correlated with nitrate (r^2=0.86), implying common mechanisms in their variability, possibly linked with the partitioning between

the gas and particulate phases. The poor correlation with CO (r^2=0.4) and BC (r^2=0.35) implies that SV-OOA may, to some extent, partially originate from a combustion source. LV-OOA shows good correlation with sulfate (r^2=0.62) and ammonium (r^2=0.63), consistent with the regional character of this factor. Results from the trajectory cluster analysis (Figure 8) show that enhanced

435   LV-OOA levels are related to air masses originating from Eastern Europe and the Black Sea region, which have both been identified as the main areas of influence for secondary aerosols that are regionally processed and transported to Athens (Gerasopoulos et al., 2011; Grivas et al., 2018). The regional character of LV-OOA is confirmed by high concentrations associated with increased wind speeds (Figure SF.20), especially those that originate from the Northern sector. These results

440   (presented in the Figure for the full dataset) are contrasted with HOA which displays a much less diffuse spread, due to the intensity of local emissions (mainly traffic in the center of Athens). The distant signal for LV-OOA to the SE direction could possibly be associated to processed aerosol deriving from shipping activity (Petit et al., 2014) in the Aegean Sea.

Primary fossil fuel emissions (HOA) are very low during summer exhibiting a fivefold

445   decrease compared to the cold season, as in July and August most of the Athenians leave for their summer vacations, thus reducing local traffic. Concentrations peak around 7:00 and after 19:00 LT that corresponds to the early morning and evening rush hours in downtown Athens. COA exhibits a slight hump during lunch hours (13:00-15:00 LT) where concentrations rise to 65% of the daily COA average after the morning minimum of around 50%, also seen in the relative

450   contribution of the factor, while a large night-time peak is present at around 22:00 LT. This late peak, three times higher than the daily average value, is consistent with the late dinner hours and operation of grill houses and restaurants in central Athens. SV-OOA exhibits 40% higher concentrations during night-time compared to the SV-OOA daily average, which apart from boundary layer dynamics may also be attributed to the condensation of semi-volatile compounds,

455   as also implied by the excellent correlation of the factor with nitrate. During daytime, following the sharp decrease from the night time maxima, concentrations remain for some hours (10:00 to 14:00) close to 80% of the daily average before declining further in the afternoon. Finally, LV-OOA exhibits a peak during mid-day, consistent with increased photochemical processes during the peak of solar radiation intensity (Figure SF.1) that lead to further organic aerosol oxidation.

460   In summary, during the warm period, the vast majority (more than 80%) of organic aerosol in the area is linked to secondary organic aerosol formation. The semi-volatile product is of mixed

origin, linked to quick atmospheric processes, within a few hours, such as photochemistry of primary sources, like biogenic emissions from vegetation, traffic emissions, or probably to a lesser extent regional biomass burning. This last assumption could be supported by the fact that OOA linked to aged BBOA has been reported in regional background sites in Greece (Bougiatioti et al., 2014) and elsewhere (Minguillon et al., 2015), as well as by the fact that during the warm season, air masses which mostly originate from the north, northeastern sector, carry pollutants from the Balkans and around the Black Sea, areas heavily impacted by wildfires from July to September (Sciare et al., 2008) (Fig. SF.21). On the contrary, the low-volatility product is the result of more extensive oxidation of organic aerosol in the area, within a few days, and has, thus, exhibits a more regional character.

Cold period: In this period, the selected solution is a three factor constrained run (HOA using α =0.1, COA using α =0.2, BBOA using α =0.4) and consists of five factors: BBOA (biomass burning OA), HOA, COA, SV-OOA and LV-OOA. The solution for winter 2016-17 is presented (Fig. 6), while the respective solutions for winter 2013-14 and 2015-16 are provided in the supplementary material (Fig. SF.13). The time series of the five PMF factors for winter 2016-17 are shown in Figure 6 along with their diurnal variability and the hourly contribution of each factor.

In terms of affinity with RFPs found in the literature, HOA for the cold season in this study is found to exhibit excellent correlations with spectra obtained during the same season in earlier studies in Athens as well as other Greek cities (e.g. Patras) (Florou et al., 2017) and also with HOA factors obtained in different environments, a fact also observed for the warm season obtained spectrum (Fig. SF.15). COA is excellently correlated with COA from Florou et al. (2017) in both Athens and Patras as well as with COA measured by Kaltsonoudis et al. (2017) (Fig. SF.16). When calculating the elemental ratios based on the study of Canagaratna et al. (2015) the O:C ratio for COA is 0.18, which is in accordance with the value of 0.11 derived for COA at the same site by Florou et al. (2017). BBOA exhibits high correlation with factors form Zurich, Paris and Finokalia as summarized in Figure SF.17, while excellent correlation is found when compared to BBOA found in Bologna, earlier studies in Athens and in Patras. Once more, the calculated O:C ratio for BBOA is 0.25, which is in accordance with the value of 0.27 derived for BBOA at the same site by Florou et al. (2017). The SV-OOA spectrum exhibits high correlation with the average SV-OOA from Ng et al. (2011b), as well as with the IEPOX-OA from Budisulistiorini et al. (2013)

(r^2=0.80 in both cases), as isoprene main oxidation products such as methyl vinyl ketone and methacrolein are often used as biomass burning tracers (Santos et al., 2017). Similar correlation is also found with IEPOX-OA and SV-OOA during the winter 2015-16 campaign. The factor exhibits high correlation with SV-OOA from wintertime in Paris (Crippa et al., 2013) and SV-OOA from Hyytiälä (Äijälä et al., 2017)(Fig. SF.18). Finally, LV-OOA records an excellent correlation with the LV-OOA from Crippa et al. (2014), the average LV-OOA from Ng et al. (2011b), LV-OOA from Zurich during winter (Lanz et al., 2008) as well as with the oxidized OOA found in the extended area (Finokalia) (Bougiatioti et al., 2014) (Fig. SF.19).

Since the identification of BBOA is mainly based on the two fragments of m/z 60 and 73, considered as the "fingerprint" fragments of levoglucosan and biomass burning tracers, BBOA exhibits indeed excellent correlation with these two fragments (r^2=0.94 and 0.9, respectively). Nss-K^+ is also proposed as a very good tracer for biomass burning and as is reported by Fourtziou et al. (2017), it shows a significant correlation with BC coming from wood burning (BC_{wb}), during wintertime in Athens. Consequently, the time series of nss-K^+ provided by PILS-IC and m/z 60 are studied together. It appears that during both winters (2013-14 and 2016-17) for which nss-K^+ data is available, m/z 60 is in very good agreement with nss-K^+ (r^2=0.85) (Figure 7a). Furthermore, BBOA is highly correlated with BC_{wb} (r^2=0.77), exhibits good correlation with nss-K^+ (r^2=0.55) and with CO (r^2=0.51). SV-OOA correlates excellently with both wood burning "fingerprint" fragments of m/z 60 and 73 (r^2=0.99 for both), highly with BC_{wb} (r^2=0.90) and CO (r^2=0.73) (Figure 7b) while exhibiting good correlation with nss-K^+ (r^2=0.55), demonstrating the direct link between SV-OOA and primary combustion sources (mainly biomass burning) (Table ST.2). It can be seen in Figure SF.21, that increased concentrations of both BBOA and SV-OOA are linked to air masses originating from Northern and Eastern Europe. During wintertime, these flow categories are associated with the prevalence of synoptic-scale northern winds and a decline in temperature in the area, leading to the appearance of PM episodes due to local combustion for residential heating (Paschalidou et al., 2015). The input of local sources confined in the Athens basin and in the vicinity of the sampling site is indicated by results of the wind analysis presented in Figure SF.20. Markedly enhanced levels are associated with weak or stagnant conditions. Results are contrasted with those of Grivas et al. (2018) who at a moderately populated area in the eastern part of the basin found that local biomass burning emissions played a less important role than advections from the northern part of the area. In the present case, in the densely populated

center of Athens this effect is less apparent. The locality of wood burning aerosols in dense residential areas in Athens has also been indicated by Argyropoulos et al. (2017).

Comparison of the HOA time series with BC and CO yields a good correlation (r^2=0.65 and r^2=0.65 respectively). The factor correlates consistently better with BC_{ff} than with BC_{wb} (e.g. for the 2016 – 2017 r^2 is 0.60 versus 0.52 respectively). Correlation of COA with nss-K^+ and chloride (0.3<r^2<0.4) could indicate a minor influence from emissions derived from biomass burning in meat-cooking (Akagi et al. 2011; Kaltsonoudis et al., 2017). Finally, LV-OOA showed a good correlation with ammonium (r^2=0.58), nitrate (r^2=0.61), nss- K^+ (r^2=0.4) and m/z 73 (r^2=0.51), demonstrating that part of the very oxidized OA during wintertime may also originate from combustion sources as well.

Therefore, during the cold period, the organic aerosol in the area linked to secondary organic aerosol formation contributes around 65% to the total organic fraction. In contrast to summer, the semi-volatile product seems to be linked to the fast oxidation of primary combustion sources (e.g. BBOA), which is also reflected on its diurnal variability (Fig. 6) and also on the strong correlations with external tracers of primary combustion (see Table ST.2). Its affinity to biomass burning tracers points out that the largest part of it originates from the fast oxidation of BBOA. The low-volatility product is in this case likely of more local than long-range transport nature, as also highlighted by the almost two-fold higher values during night-time.

The diurnal cycles of the five factors are shown in Figure 6. HOA, originating from fossil fuel combustion, exhibits maximum values during night, associated with combustion from central heating, and presents a secondary peak at 09:00 coinciding with the early morning traffic rush hour. The association of the factor to local primary emissions is also corroborated by the wind analysis plots (Figure SF.20). The dependence of HOA on wind speed and direction is similar between cold and warm seasons. The concentration vs. wind speed distribution, displays a wind dilution effect and is characteristic for traffic-related fine particles in Athens (Chaloulakou et al., 2003; Kassomenos et al., 2012).

COA has similar winter and summer diurnal profiles with a moderate hump, with concentrations rising form 30% to 60% of the daily average during lunch hours (12-15:00 LT) and a large night-time peak (approx. 22:00 LT), partly controlled by the decrease of the planetary boundary layer, but also owing to the expected increase in the activity of numerous restaurants in the area. A similar diurnal cycle for COA has been reported by Florou et al. (2017). BBOA is

characterized by a pronounced diurnal cycle with peaking values during night-time, associated with the production of this component in the evening by combustion for heating purposes. SV-OOA exhibits the largest diurnal amplitude, with night-time values being almost 6-fold higher compared to daytime. A plateau, with concentrations of SVOOA being around 50% of the daily average value, following the sharp decline after midnight, is observed during the morning traffic rush hour, before another decline occurs until the daily minimum is reached at 14:00, demonstrating the possibility of the factor's provenance from the oxidation of freshly-emitted primary combustion organic aerosol. Finally, LV-OOA also exhibits 2-fold higher values during night compared to daytime. It has a, similar to the SV-OOA factor behavior, with a secondary peak at 10:00, followed by a 1 – hour lag the morning traffic rush hour, showing once more that part of the low volatility OA may also originate from the fast oxidation of primary combustion source, as also implied by its correlation with combustion tracers.

Table 2 sums up the contribution of each one of the 5 identified factors during the three studied winters. Overall, during wintertime BBOA constitutes around 10% of the total organic fraction. Based on the diurnal variability of this factor, its contribution is more pronounced during night-time, when concentrations are 4-fold or higher than the daytime ones, matching emissions from fossil fuel combustion represented by the HOA factor incorporating both traffic and heating oil combustion. Even though an exact mechanism has yet to be established, our assumption that the larger part of the semi-volatile OOA (SV-OOA) comes from the rapid oxidation of freshly emitted BBOA through processes which involve nitrate radicals and/or heterogeneous reactions, appears justified via the excellent correlations with biomass burning tracers as well when considering similar assessments found in other studies (Lathem et al., 2013; Cubison et al., 20011; Bougiatioti et al., 2014). In this manner the overall contribution of biomass burning becomes even more significant. Given that SV-OOA contributes around 30% to the organic mass, it is evident that during wintertime, biomass burning may contribute almost half of the total organic aerosol, with this contribution maximizing during night-time. More specifically, for BBOA the lowest contribution during daytime is 5.5% reaching a maximum of 27.5% during night (Figure 6). The same applies to SV-OOA with daytime minimum contribution of 13.8% and night-time maximum of 34.9%. What is also very important is the fact that even though the winter and summer mass spectra of SV-OOA have some similarities (r^2=0.83), there are also differences, especially in the origin of this component, as during winter the majority is linked to the oxidation of primary

combustion sources, while during summer the absence of a significant correlation with BC or nss-K^+ implies the presence of different sources, both anthropogenic (but not biomass burning) and possibly biogenic.

4. Summary and conclusions

High temporal-resolution measurements were conducted for an entire year (plus two, two-month duration, intensive measurement campaigns during wintertime) at an urban background site in Athens, using an ACSM, a PILS-IC system and an aethalometer, in excess to routine pollution measurements. During the 16 – month measurement period, several pollution events with PM_1 concentrations reaching as high as 220 μg m^{-3} were recorded, all encountered during wintertime nights. In these cases, organics contributed the largest fraction to the submicron particulate mass, with overall contribution during wintertime reaching 50%, followed by sulfate (~20%) and BC (~14%). Within a typical winter day, organics, BC and nitrate double their concentrations during night-time. The increase of the first two can be attributed to emissions linked with domestic heating while nitrate exhibits higher concentrations due to the combined effect of decreased temperature and aerosol acidity, favoring partitioning in the aerosol phase. During summer, organics, BC and nitrate concentrations are significantly lower while sulfate and ammonium levels are increased. Organics are once more the main aerosol constituent contributing by 46%, followed by sulfate (30.5%), ammonium (8.3%) and BC (8%). Within a typical summer day, ammonium and sulfate concentrations peak at about 14:00 LT (UTC+2), consistent with secondary aerosol formation.

Organics, nitrate, chloride and BC exhibited a clear seasonal cycle with maximum during winter and minimum during summer. Sulfate and ammonium exhibited the opposite cycle, as a result of enhanced photochemistry, limited precipitation and higher regional transport.

Based on the source apportionment of the organic aerosol, four factors were identified during summer, namely hydrocarbon-like OA (HOA), cooking-like OA (COA), semi-volatile oxygenated OA (SV-OOA) and low-volatility OA (LV-OOA), and five factors during winter, the same as in summer with the addition of primary biomass burning emissions (BBOA). During summer, HOA makes up 4.3% of the total organic fraction, COA around 10%, and the rest is linked to secondary organics (SV-OOA and LV-OOA). HOA has peaking values during the morning traffic rush hour, and COA mainly during night-time. SV-OOA exhibits two-fold higher concentrations during night-time while LV-OOA exhibits a peak during mid-day, consistent with

photochemical processes. The semi-volatile product is clearly of mixed origin, linked to quick atmospheric processing within a few hours, of VOCs emitted from primary sources like vegetation, traffic and to some limited extent to processed regional biomass burning. The low-volatility product, on the other hand, is the result of more excessive oxidation, in the order of several days, having thus a more regional character.

Combining the results from the three different winter campaigns, HOA accounts for almost 13% of the organic fraction, COA around 10%, BBOA 10%, SV-OOA 22% and LV-OOA 45%. All constituents exhibit significantly higher concentrations during night-time, with HOA being also linked to primary emissions by heating oil combustion from central heating units and presenting a secondary peak during the morning traffic rush hour. COA has a similar diurnal profile to the one observed during summer. BBOA is also characterized by a pronounced diurnal cycle with peaking values during night from combustion for heating. SV-OOA has almost 6-fold higher concentrations during night, consistent with its link to the oxidation of primary combustion sources, while even LV-OOA exhibits almost 2-fold higher concentrations during night. In contrast to summer, the semi-volatile product during winter has a very clear origin, linked to the fast oxidation of primary combustion sources (HOA and BBOA) with BBOA being the major source, due to the affinity of SV-OOA with biomass burning tracers. Part of the LV-OOA, as well, could originate from the extensive oxidation of the local primary combustion sources, showing that LV-OOA during winter is of more local than regional character.

Concluding, it is clear that organic aerosol constitutes a large fraction of submicron aerosol throughout the year, in the urban environment of Athens. During wintertime, a large part of this OA, as high as 50%, originates from combustion sources for heating purposes, such as biomass burning and diesel oil fueled central heating , causing significant air quality deterioration. Night-time contribution of BBOA is 7-fold higher than the one during day, while the respective contribution of SV-OOA is increased by a factor of 2.6. Given that during wintertime, fine PM concentrations reach up to 220 $\mu g\ m^{-3}$, the significance of these sources contribution becomes even more striking, demonstrating the necessity for strategic, long-term mitigation actions.

Acknowledgments

I. Stavroulas and N. Mihalopoulos acknowledge support by the State Scholarship Foundation ("IKY Fellowships of Excellence for Postgraduate Studies in Greece -Siemens Programme, 2016-2017"), in the framework of the Hellenic Republic-Siemens Settlement Agreement. The authors would also like to acknowledge support from Francesco Canonaco and Andre Prévôt from PSI, who developed SoFi and provided valuable input related to Positive Matrix Factorization. This study contributes to ChArMEx work package 1 on emissions and sources.

References

Äijälä, M., Heikkinen, L., Fröhlich, R., Canonaco, F., Prévôt, A. S. H., Junninen, H., Petäjä, T., Kulmala, M., Worsnop, D., and Ehn, M.: Resolving anthropogenic aerosol pollution types – deconvolution and exploratory classification of pollution events, Atmos. Chem. Phys., 17, 3165-3197, doi:10.5194/acp-17-3165-2017, 2017.

Akagi, S. K., Yokelson, R. J., Wiedinmyer, C., Alvarado, M. J., Reid, J. S., Karl, T., Crounse, J. D., and Wennberg, P. O.: Emission factors for open and domestic biomass burning for use in atmospheric models, Atmos. Chem. Phys., 11, 4039-4072, https://doi.org/10.5194/acp-11-4039-2011, 2011.

Alexiou, D., Kokkalis, P., Papayannis, A., Rocadenbosch, F., Argyrouli, A., Tsaknakis, G. and Tzanis, C.G.: Planetary boundary layer height variability over athens, greece, based on the synergy of raman lidar and radiosonde data: Application of the kalman filter and other techniques (2011-2016), EPJ Web of Conferences, Vol. 176, p. 06007, EDP Sciences, 2018.

Aurela, M., Saarikoski, S., Niemi, J.V., Canonaco, F., Prevot, A.S.H., Frey, A., Carbone, S., Kousa, A., and Hillamo, R.: Chemical and source characterization of submicron particles at residential and traffic sites in the Helsinki Metropolitan Area, Finland, Aerosol Air Qual. Res., 15, 1213-1226, doi: 10.4209/aaqr.2014.11.0279, 2015.

Argyriou A, Kassomenos P, Lykoudis S. On the methods for the delimitation of seasons. Water Air Soil Pollut Focus, 2004;4:65–74.

Argyropoulos, G., Samara, C., Diapouli, E., Eleftheriadis, K., Papaoikonomou, K., and Kungolos, A.: Source apportionment of PM_{10} and $PM_{2.5}$ in major urban Greek agglomerations using a hybrid source-receptor modeling process, Sci. Total Environ., 601-602, 906-917, doi:10.1016/j.scitotenv.2017.05.088, 2017.

Asimakopoulos, D.N., Helmis, C.G. and Michopoulos, J.: Evaluation of SODAR methods for the determination of the atmospheric boundary layer mixing height, Meteorology and Atmospheric Physics, 85(1-3), 85-92, doi:10.1007/s00703-003-0036-9, 2004.

680 Bahreini, R., Keywood, M.D., Ng, N.L., Varutbangkul, V., Gao, S., Flagan, R.C., Seinfeld, J.H., Worsnop, D.R. and Jimenez, J.L. Measurements of secondary organic aerosol from oxidation of cycloalkenes, terpenes, and m-xylene using an Aerodyne aerosol mass spectrometer, Environmental science & technology, 39(15), 5674-5688., doi:10.1021/es048061a, 2005

685 Bougiatioti, A., Stavroulas, I., Kostenidou, E., Zarmpas, P., Theodosi, C., Kouvarakis, G., Canonaco, F., Prevot, A.S.H., Nenes, A., Pandis, S.N., Mihalopoulos, N.: Processing of biomass-burning aerosol in the eastern Mediterranean during summertime, Atmos. Chem. Phys. 14 (9), 4793-4807, doi:10.5194/acp-14-4793-2014, 2014.

Budisulistiorini, S.H., Canagaratna, M.R., Croteau, P.L., Marth, W.J., Baumann, K., Edgerton, 690 E.S., Shaw, S.L., Knipping, E.M., Worsnop, D.R., Jayne, J.T., Gold, A., and Surratt, J.D.: Real-time continuous characterization of secondary organic aerosol derived from isoprene epoxydiols in downtown Atlanta, Georgia using the Aerodyne Aerosol Chemical Speciation Monitor, Environ. Sci. Technol., 47 (11), 5686-5694, doi:10.1021/es400023n, 2013.

Canagaratna, M. R., Jimenez, J. L., Kroll, J. H., Chen, Q., Kessler, S. H., Massoli, P., Hildebrandt 695 Ruiz, L., Fortner, E., Williams, L. R., Wilson, K. R., Surratt, J. D., Donahue, N. M., Jayne, J. T., and Worsnop, D. R.: Elemental ratio measurements of organic compounds using aerosol mass spectrometry: characterization, improved calibration, and implications, Atmos. Chem. Phys., 15, 253-272, doi:10.5194/acp-15-253-2015, 2015.

Canonaco, F., Crippa, M., Slowik, J. G., Baltensperger, U., and Prévôt, A. S. H.: SoFi, an IGOR- 700 based interface for the efficient use of the generalized multilinear engine (ME-2) for the source apportionment: ME-2 application to aerosol mass spectrometer data, Atmos. Meas. Tech., 6, 3649-3661, doi:10.5194/amt-6-3649-2013, 2013.

Canonaco, F., Slowik, J. G., Baltensperger, U., and Prévôt, A. S. H.: Seasonal differences in oxygenated organic aerosol composition: implications for emissions sources and factor 705 analysis, Atmos. Chem. Phys., 15, 6993-7002, https://doi.org/10.5194/acp-15-6993-2015, 2015.

Carslaw, D.C., and Ropkins, K.: Openair - an R package for air quality data analysis, Environ. Model. Softw., 27-28, 52-61, doi:10.1016/j.envsoft.2011.09.008, 2012.

Cavalli F., Viana M., Yttri K.E., Genberg J., Putaud J.P.: Toward a standardised thermal–optical protocol for measuring atmospheric organic and elemental carbon: The EUSAAR protocol, Atmos. Meas. Techniques, 3, 79-89, doi:10.5194/amt-3-79-2010, 2010.

Chaloulakou, A., Kassomenos, P., Spyrellis, N., Demokritou, P., and Koutrakis, P.: Measurements of PM_{10} and $PM_{2.5}$ particle concentrations in Athens, Greece, Atmos. Environ., 37, 649–660, doi: 10.1016/S1352-2310(02)00898-1, 2003.

Crippa, M., DeCarlo, P. F., Slowik, J. G., Mohr, C., Heringa, M. F., Chirico, R., Poulain, L., Freutel, F., Sciare, J., Cozic, J., Di Marco, C. F., Elsasser, M., Nicolas, J. B., Marchand, N., Abidi, E., Wiedensohler, A., Drewnick, F., Schneider, J., Borrmann, S., Nemitz, E., Zimmermann, R., Jaffrezo, J.-L., Prévôt, A. S. H., and Baltensperger, U.: Wintertime aerosol chemical composition and source apportionment of the organic fraction in the metropolitan area of Paris, Atmos. Chem. Phys., 13, 961-981, doi: 10.5194/acp-13-961-2013, 2013.

Crippa, M., Canonaco, F., Lanz, V. A., Äijälä, M., Allan, J. D., Carbone, S., Capes, G., Ceburnis, D., Dall'Osto, M., Day, D. A., DeCarlo, P. F., Ehn, M., Eriksson, A., Freney, E., Hildebrandt Ruiz, L., Hillamo, R., Jimenez, J. L., Junninen, H., Kiendler-Scharr, A., Kortelainen, A.-M., Kulmala, M., Laaksonen, A., Mensah, A. A., Mohr, C., Nemitz, E., O'Dowd, C., Ovadnevaite, J., Pandis, S. N., Petäjä, T., Poulain, L., Saarikoski, S., Sellegri, K., Swietlicki, E., Tiitta, P., Worsnop, D. R., Baltensperger, U., and Prévôt, A. S. H.: Organic aerosol components derived from 25 AMS data sets across Europe using a consistent ME-2 based source apportionment approach, Atmos. Chem. Phys., 14, 6159-6176, doi:10.5194/acp-14-6159-2014, 2014.

Cubison, M. J., Ortega, A. M., Hayes, P. L., Farmer, D. K., Day, D., Lechner, M. J., Brune, W. H., Apel, E., Diskin, G. S., Fisher, J. A., Fuelberg, H. E., Hecobian, A., Knapp, D. J., Mikoviny, T., Riemer, D., Sachse, G. W., Sessions, W., Weber, R. J., Weinheimer, A. J., Wisthaler, A., and Jimenez, J. L.: Effects of aging on organic aerosol from open biomass burning smoke in aircraft and laboratory studies, Atmos. Chem. Phys., 11, 12049–12064, doi:10.5194/acp-11-12049-2011, 2011.

Cusack M, Alastuey A, Pérez N, Pey J, Querol X.: Trends of particulate matter ($PM_{2.5}$) and chemical composition at a regional background site in the Western Mediterranean over the last

nine years (2002-2010), Atmos. Chem. Phys., 12, 8341–8357, doi:10.5194/acp-12-8341-2012, 2012.

Drinovec, L., Močnik, G., Zotter, P., Prévôt, A. S. H., Ruckstuhl, C., Coz, E., Rupakheti, M., Sciare, J., Müller, T., Wiedensohler, A., and Hansen, A. D. A.: The "dual-spot" Aethalometer: an improved measurement of aerosol black carbon with real-time loading compensation, Atmos. Meas. Tech., 8, 1965-1979, doi: 10.5194/amt-8-1965-2015, 2015.

EEA, 2017. Air quality in Europe — 2017 report, No 13/2017. European Environment Agency. ISSN 1725-917.El Haddad, I., D'Anna, B., Temime-Roussel, B., Nicolas, M., Boreave, A., Favez, O., Voisin, D., Sciare, J., George, C., Jaffrezo, J.-L., Wortham, H., and Marchand, N.: Towards a better understanding of the origins, chemical composition and aging of oxygenated organic aerosols: case study of a Mediterranean industrialized environment, Marseille, Atmos. Chem. Phys., 13, 7875-7894, 2013.

Florou, K., Papanastasiou, D. K., Pikridas, M., Kaltsonoudis, C., Louvaris, E., Gkatzelis, G. I., Patoulias, D., Mihalopoulos, N., and Pandis, S. N.: The contribution of wood burning and other pollution sources to wintertime organic aerosol levels in two Greek cities, Atmos. Chem. Phys., 17, 3145-3163, doi: 10.5194/acp-17-3145-2017, 2017.

Fourtziou, L., Liakakou, E., Stavroulas, I., Theodosi, C., Zarmpas, P., Psiloglou, B., Sciare, J., Maggos, T., Bairachtari, K., Bougiatioti, A. and Gerasopoulos, E.: Multi-tracer approach to characterize domestic wood burning in Athens (Greece) during wintertime. Atmospheric Environment, 148, 89-101, doi:10.1016/j.atmosenv.2016.10.011, 2017.

Gerasopoulos, E., Amiridis, V., Kazadzis, S., Kokkalis, P., Eleftheratos, K., Andreae, M.O., Andreae, T.W., El-Askary, H., Zerefos, C.S.: Three-year ground based measurements of aerosol optical depth over the Eastern Mediterranean: The urban environment of Athens, Atmos. Chem. Phys. 11, 2145-2159, doi:10.5194/acp-11-2145-2011 2011.

Gilardoni, S., Massoli, P., Paglione, M., Giulianelli, L., Carbone, C., Rinaldi, M., Decesari, S., Sandrini, S., Costabile, F., Gobbi, G.P. and Pietrogrande, M.C.: Direct observation of aqueous secondary organic aerosol from biomass-burning emissions. Proceedings of the National Academy of Sciences, 113(36), pp.10013-10018, 2016.

Gratsea, M., Liakakou, E., Mihalopoulos, N., Adamopoulos, A., Tsilibari, E., and Gerasopoulos, E.: The combined effect of reduced fossil fuel consumption and increasing biomass

combustion on Athens' air quality, as inferred from long term CO measurements, Sci. Tot. Environ., 592, 115-123, doi:10.1016/j.scitotenv.2017.03.045, 2017.

Grivas, G., Cheristanidis, S., and Chaloulakou, A.: Elemental and organic carbon in the urban environment of Athens. Seasonal and diurnal variations and estimates of secondary organic carbon, Sci. Tot. Environ., 414, 535-545, doi:10.1016/j.scitotenv.2011.10.058, 2012.

Grivas, G., Cheristanidis, S., Chaloulakou, A., Koutrakis, P., and Mihalopoulos, N.: Elemental composition and source apportionment of fine and coarse particles at traffic and urban background locations in Athens, Greece, Aerosol and Air Qual. Res., 18, 1642-1659, doi: 10.4209/aaqr.2017.12.0567, 2018.

Guo, H., Sullivan, A.P., Campuzano-Jost, P., Schroder, J.C., Lopez-Kilfiker, F.D., Dibb, J.E., Jimenez, J.L., Thornton, J.A., Brown, S.S., Nenes, A., and Weber, R.J.: Fine particle pH and the partitioning of nitric acid during winter in the northeastern United States, J. Geophys. R. Atmos., 121, 10355-10376, doi:10.1002/2016JD025311, 2016.

Harrison, D.; Hunter, M. C.; Lewis, A. C.; Seakins, P. W.; Bonsang, B.; Gros, V.; Kanakidou, M .; Touaty, M.; Kavouras, I.; Mihalopoulos, N.; Stephanou, E.; Alves, C.; Nunes, T.; Pio, C.: Ambient isoprene and monoterpene concentrations in a Greek fir (Abies Borisii-regis) forest. Reconciliation with emissions measurements and effects on measured OH concentrations, Atmos. Environ., Vol. 35, Issue 27, p. 4699-4711, 2001.

Hatch, L.E., Jessie M. Creamean, Andrew P. Ault, Jason D. Surratt, Man Nin Chan, John H. Seinfeld, Eric S. Edgerton, Yongxuan Su, and Kimberly A. Prather: Measurements of Isoprene-Derived Organosulfates in Ambient Aerosols by Aerosol Time-of-Flight Mass Spectrometry—Part 2: Temporal Variability and Formation Mechanisms, Environ. Sci. Technol., 45 (20), 8648-8655, doi: 10.1021/es2011836, 2011.

Ito, K., Mathes, R., Ross, Z., Nádas, A., Thurston, G., and Matte, T.: Fine particulate matter constituents associated with cardiovascular hospitalizations and mortality in New York City, Environ. Health Perspect., 119, 467-473, doi:10.1289.ehp.1002667, 2011.

Jayne, J.T., D.C. Leard, X. Zhang, P. Davidovits, K.A. Smith, C.E. Kolb, and D.R.Worsnop, Development of an Aerosol Mass Spectrometer for Size and Composition. Analysis of Submicron Particles, Aerosol Science and Technology, 33, 49-70, doi:10.1080/027868200410840, 2000.

Jimenez, J. L., Canagaratna, M. R., Donahue, N. M., Prevot, A. S.H., Zhang, Q., Kroll, J. H., DeCarlo, P. F., Allan, J. D., Coe, H., Ng, N. L., Aiken, A. C., Docherty, K. D., Ulbrich, I. M., Grieshop, A. P., Robinson, A. L., Duplissy, J., Smith, J. D., Wilson, K. R., Lanz, V. A., Hueglin, C., Sun, Y. L., Tian, J., Laaksonen, A., Raatikainen, T., Rautiainen, J., Vaattovaara, P., Ehn, M., Kulmala, M., Tomlinson, J. M., Collins, D. R., Cubison, M. J., Dunlea, E. J., Huffman, J. A., Onasch, T. B., Alfarra, M. R., Williams, P. I., Bower, K., Kondo, Y., Schneider, J., Drewnick, F., Borrmann, S., Weimer, S., Demerjian, K., Salcedo, D., Cottrell, L., Griffin, R., Takami, A., Miyoshi, T., Hatakeyama, S., Shimono, A., Sun, J. Y., Zhang, Y. M., Dzepina, K., Kimmel, J.R., Sueper, D., Jayne, J. T., Herndon, S. C., Trimborn, A. M., Williams, L. R.,Wood, E. C., Kolb, C. E., Baltensperger, U., and Worsnop, D. R.: Evolution of organic aerosol in the atmosphere, Science, 326, 1525–1529, doi:10.1126/science.1180353, 2009.

Kalogridis, A.-C., Vratolis, S., Liakakou, E., Gerasopoulos, E., Mihalopoulos, N., and Eleftheriadis, K.: Assessment of wood burning versus fossil fuel contribution to wintertime black carbon and carbon monoxide concentrations in Athens, Greece, Atmos. Chem. Phys. Discuss., https://doi.org/10.5194/acp-2017-854, in review, 2017.

Kaltsonoudis, C., Kostenidou, E., Louvaris, E., Psichoudaki, M., Tsiligiannis, E., Florou, K., Liangou, A., and Pandis, S. N.: Characterization of fresh and aged organic aerosol emissions from meat charbroiling, Atmos. Chem. Phys., 17, 7143-7155, doi: 10.5194/acp-17-7143-2017, 2017.

Kanakidou, M., Mihalopoulos, N., Kindap, T., Im, U., Vrekoussis, M., Gerasopoulos, E., Dermitzaki, E., Unal, A., Koçak, M., Markakis, K., Melas, D., Kouvarakis, G., Youssef, A.F., Richter, A., Hatzianastassiou, N., Hilboll, A., Ebojie, F., Wittrock, F., Von Savigny, C., Burrows, J.P., Ladstaetter-Weissenmayer, A., Moubasher, H.: Megacities as hot spots of air pollution in the East Mediterranean, Atmos. Environ. 45, 1223-1235, doi: 10.1016/j.atmosenv.2010.11.048, 2011.

Kassomenos, P., Kotroni, V., and Kallos, G.: Analysis of climatological and air quality observations from Greater Athens Area, Atmos. Environ., 29, 3671-3688, doi:10.1016/1352-2310(94)00358-R, 1995.

Kassomenos, P., Vardoulakis, S., Chaloulakou, A., Grivas, G., Borge, R., and Lumbreras, J: Levels, sources and seasonality 30 of coarse particles (PM_{10}-$PM_{2.5}$) in three European capitals

- Implications for particulate pollution control, Atmos. Environ., 54, 337-347, 10.1016/j.atmosenv.2012.02.051, 2012.

Kazadzis, S., Founda, D., Psiloglou, B. E., Kambezidis, H., Mihalopoulos, N., Sanchez-Lorenzo, A., Meleti, C., Raptis, P. I., Pierros, F., and Nabat, P.: Long-term series and trends in surface solar radiation in Athens, Greece, Atmos. Chem. Phys., 18, 2395-2411, doi: 10.5194/acp-18-2395-2018, 2018.

Klemm, R.J., Thomas, E.L., and Wyzga, R.E.: The impact of frequency and duration of air quality monitoring: Atlanta, GA, data modeling of air pollution and mortality, J. Air Waste Manage. Assoc., 61, 1281-1291, doi:10.1080/10473289.2011.617648, 2011.

Kostenidou, E., Florou, K., Kaltsonoudis, C., Tsiflikiotou, M., Vratolis, S., Eleftheriadis, K., and Pandis, S. N.: Sources and chemical characterization of organic aerosol during the summer in the eastern Mediterranean, Atmos. Chem. Phys., 15, 11355-11371, doi:10.5194/acp-15-11355-2015, 2015.

Lanz, V. A., Alfarra, M. R., Baltensperger, U., Buchmann, B., Hueglin, C., Szidat, S., Wehrli, M. N., Wacker, L., Weimer, S., Caseiro, A., Puxbaum, H., and Prevot, A. S. H.: Source attribution of submicron organic aerosols during wintertime inversions by advanced factor analysis of aerosol mass spectra, Environ. Sci. Technol., 42 (1), 214–220, doi:10.1021/es0707207, 2008.

Lathem, T. L., Beyersdorf, A. J., Thornhill, K. L., Winstead, E. L., Cubison, M. J., Hecobian, A., Jimenez, J. L., Weber, R. J., Anderson, B. E., and Nenes, A.: Analysis of CCN activity of Arctic aerosol and Canadian biomass burning during summer 2008, Atmos. Chem. Phys., 13, 2735–2756, doi:10.5194/acp-13-2735-2013, 2013.

Levy, J.I., Diez, D., Dou, Y., Barr, C.D., and Dominici, F.: A meta-analysis and multisite time-series analysis of the differential toxicity of major fine particulate matter constituents, Am. J. Epidemiol., 175, 1091-1099, doi:10.1093/aje/kwr457, 2012.

Li, J., Gehui Wang, Can Wu, Cong Cao, Yanqin Ren, Jiayuan Wang, Jin Li, Junji Cao, Limin Zeng & Tong Zhu, 2018. Characterization of isoprene-derived secondary organic aerosol at a rural site in North China Plain with implications for anthropogenic pollution effects, Scientific Reports, 8, Article number 535, 2018.

Mariani, R.L. and de Mello, W.Z.: $PM_{2.5-10}$, $PM_{2.5}$ and associated water-soluble inorganic species at a coastal urban site in the metropolitan region of Rio de Janeiro, Atmos. Environ., 41, 2887-2892, doi:10.1016/j.atmosenv.2006.12.009, 2007.

860 Markou, M.T., and Kassomenos, P.: Cluster analysis of five years of back trajectories arriving in Athens, Greece, Atmos. Res., 98, 438-457, doi:10.1016/j.atmosres.2010.08.006, 2010.

Middlebrook, A. M., Bahreini, R., Jimenez, J. L., and Canagaratna, M. R.: Evaluation of Composition-Dependent Collection Efficiencies for the Aerodyne Aerosol Mass Spectrometer using Field Data, Aerosol Sci. Technol., 46, 258–271, doi: 10.1080/02786826.2011.620041,
865 2012.

Minguillón, M.C., Pérez, N., Marchand, N., Bertrand, A., Temime-Roussel, B., Agrios, K., Szidat, S., Van Drooge, B., Sylvestre, A., Alastuey, A., Reche, C., Ripoll, A., Marco, E., Grimalt, J.O., and Querol, X.: Secondary organic aerosol origin in an urban environment: Influence of biogenic and fuel combustion precursors, Faraday Discuss., 189, 337-359,
870 doi:10.1039/c5fd00182j, 2016.

Mohr, C., DeCarlo, P. F., Heringa, M. F., Chirico, R., Slowik, J. G., Richter, R., Reche, C., Alastuey, A., Querol, X., Seco, R., Peñuelas, J., Jiménez, J. L., Crippa, M., Zimmermann, R., Baltensperger, U. and Prévôt, A. S. H.: Identification and quantification of organic aerosol from cooking and other sources in Barcelona using aerosol mass spectrometer data, Atmos.
875 Chem. Phys., 12, 1649–1665, doi:10.5194/acp-12-1649-2012, 2012.Ng, N. L., Herndon, S. C., Trimborn, A., Canagaratna, M. R., Croteau, P. L., Onasch, T. B., Sueper, D.,Worsnop, D. R., Zhang, Q., Sun, Y. L., and Jayne, J. T.: An Aerosol Chemical Speciation Monitor (ACSM) for routine monitoring of the composition and mass concentration of ambient aerosol, Aerosol Sci. Technol., 45, 780–794, doi:10.1080/02786826.2011.560211, 2011a.

880 Ng, N. L., Canagaratna, M. R., Jimenez, J. L., Zhang, Q., Ulbrich, I. M., and Worsnop, D. R.: Real-time methods for estimating organic component mass concentrations from aerosol mass spectrometer data, Environ. Sci. Technol., 45, 910–916, doi:10.1021/es102951k, 2011b.

Orsini, D.A., Ma, Y., Sullivan, A., Sierau, B., Baumann, K., Weber, R.J.: Refinements to the particle-into-liquid sampler (PILS) for ground and airborne measurements of water soluble
885 aerosol composition, Atmos. Environ. 37 (9-10), 1243-1259, doi:10.1016/S1352-2310(02)01015-4, 2003.

Ostro, B., Lipsett, M., Reynolds, P., Goldberg, D., Hertz, A., Garcia, C., Henderson, K.D. and Bernstein, L.: Long-term exposure to constituents of fine particulate air pollution and mortality: Results from the California teachers study, Environ. Health Perspect., 118, 363-369,
890 doi:10.1289/ehp.0901181, 2010.

Paatero, P. and Hopke, P.K.: Discarding or downweighting high-noise variables in factor analytic models, Analytica Chimica Acta, 490(1-2), 277-289, doi:10.1016/S0003-2670(02)01643-4, 2003.

Paatero, P. and Tapper, U.: Positive matrix factorization: A non-negative factor model with optimal utilization of error estimates of data values. Environmetrics, 5(2), 111-126, doi:10.1002/env.3170050203, 1994.

Paraskevopoulou, D., Liakakou, E., Gerasopoulos, E., Theodosi, C., Mihalopoulos, N.: Long-term characterization of organic and elemental carbon in the PM2.5 fraction: the case of Athens Greece, Atmos. Chem. Phys. 14, 13313-13325, doi:10.5194/acp-14-13313-2014, 2014.

Paraskevopoulou, D, Liakakou, E., Gerasopoulos, E., and Mihalopoulos, N.: Sources of atmospheric aerosol from long-term measurements (5years) of chemical composition in Athens, Greece, Sci. Tot. Environ., 527-528, 165-178, doi:10.1016/j.scitotenv.2015.04.022, 2015.

Park, S.S., Ondov, J.M., Harrison, D., and Nair, N.P.: Seasonal and short-term variations in particulate atmospheric nitrate in Baltimore, Atmos. Environ., 39, 2011-2020, doi:10.1016/j.atmosenv.2004.12.032, 2005.

Paschalidou, A.K., Kassomenos, P., Karanikola, P.: Disaggregating the contribution of local dispersion and long-range transport to the high PM_{10} values measured in a Mediterranean urban environment, Sci. Total Environ., 527-528, 119-125, doi: 10.1016/j.scitotenv.2015.04.094, 2015.

Pateraki, St, Asimakopoulos, D.N., Bougiatioti, A., Maggos, Th, Vasilakos, Ch, and Mihalopoulos, N.: Assessment of PM2.5 and PM1 chemical profile in a multiple-impacted Mediterranean urban area: origin, sources and meteorological dependence, Sci. Total Environ. 479, 210-220, doi:10.1016/j.scitotenv.2014.02.008, 2014.

Petit, J.-E., Favez, O., Sciare, J., Canonaco, F., Croteau, P., Močnik, G., Jayne, J., Worsnop, D., and Leoz-Garziandia, E.: Submicron aerosol source apportionment of wintertime pollution in Paris, France by double positive matrix factorization (PMF2) using an aerosol chemical speciation monitor (ACSM) and a multi-wavelength Aethalometer, Atmos. Chem. Phys., 14, 13773-13787, doi:10.5194/acp-14-13773-2014, 2014.

Petit, J.-E., Favez, O., Sciare, J., Crenn, V., Sarda-Estève, R., Bonnaire, N., Močnik, G., Dupont, J.-C., Haeffelin, M., and Leoz-Garziandia, E.: Two years of near real-time chemical

composition of submicron aerosols in the region of Paris using an Aerosol Chemical Speciation Monitor (ACSM) and a multi-wavelength Aethalometer, Atmos. Chem. Phys., 15, 2985-3005, doi: 10.5194/acp-15-2985-2015, 2015.

925 Petit, J.-E., Favez, O., Albinet, A., and Canonaco, F.: A user-friendly tool for comprehensive evaluation of the geographical origins of atmospheric pollution: wind and trajectory analyses, Environ. Model. Soft., 88, 183-187, doi: 10.1016/j.envsoft.2016.11.022, 2017.

Reyes-Villegas, E., Green, D. C., Priestman, M., Canonaco, F., Coe, H., Prévôt, A. S. H. and Allan, J. D.: Organic aerosol source apportionment in London 2013 with ME-2: exploring the solution
930 space with annual and seasonal analysis, Atmos. Chem. Phys., 16, 15545–15559, doi:10.5194/acp-16-15545-2016, 2016.

Saarikoski, S., Carbone, S., Decesari, S., Giulianelli, L., Angelini, F., Canagaratna, M., Ng, N. L., Trimborn, A., Facchini, M. C., Fuzzi, S., Hillamo, R., and Worsnop, D.: Chemical characterization of springtime submicrometer aerosol in Po Valley, Italy, Atmos. Chem. Phys.,
935 12, 8401-8421, doi:10.5194/acp-12-8401-2012, 2012.

Saffari, A., Daher, N., Samara, C., Voutsa, D., Kouras, A., Manoli, E., Karagkiozidou, O., Vlachokostas, C., Moussiopoulos, N., Shafer, M.M., Schauer, J.J., and Sioutas, C.: Increased Biomass Burning Due to the Economic Crisis in Greece and Its Adverse Impact on Wintertime Air Quality in Thessaloniki. Environmental Science & Technology, 47 (23), 13313,
940 doi:10.1021/es403847h, 2013.

Sage, A. M., Weitkamp, E. A., Robinson, A. L., and Donahue, N. M.: Evolving mass spectra of the oxidized component of organic aerosol: results from aerosol mass spectrometer analyses of aged diesel emissions, Atmos. Chem. Phys., 8, 1139-1152, doi:10.5194/acp-8-1139-2008, 2008.

945 Sandradewi, J., Prevot, A. S. H., Szidat, S., Perron, N., Lanz, V. A., Weingartner, E., and Baltensperger, U.: Using aerosol light absorption measurements for the quantitative determination of wood burning and traffic emission contributions to particulate matter, Environ. Sci. Technol., 42, 3316–3323, doi:10.1021/es702253m, 2008.

Santos, F. C., Longo, K. M., Guenther, A. B., Kim, S., Gu, D., Oram, D. E., Forster, G. L., Lee,
950 J., Hopkins, J. R., Brito, J. F., and Freitas, S. R.: Biomass burning emissions disturbances on the isoprene oxidation in a tropical forest, Atmos. Chem. Phys. Discuss., doi:10.5194/acp-2017-1083, in review, 2017.

Schneider, J., Weimer, S., Drewnick, F., Borrmann, S., Helas, G., Gwaze, P., Schmid, O., Andreae, M.O. and Kirchner, U.: Mass spectrometric analysis and aerodynamic properties of various types of combustion-related aerosol particles, Int. J. Mass Spectrom., 258, 37–49, doi:10.1016/ j.ijms.2006.07.008, 2006.

Sciare, J., Oikonomou, K., Cachier, H., Mihalopoulos, N., Andreae, M.O., Waenhaut, W., and Sarda-Estève, R.: Aerosol mass closure and reconstruction of the light scattering coefficient over the Eastern Mediterranean Sea during the MINOS campaign, Atmos. Chem. Phys., 5, 2253-2265, doi:10.5194/acp-5-2253-2005, 2005.

Sciare, J., Oikonomou, K., Favez, O., Liakakou, E., Markaki, Z., Cachier, H. and Mihalopoulos, N.: Long-term measurements of carbonaceous aerosols in the Eastern Mediterranean: Evidence of long-range transport of biomass burning, Atmos. Chem. Phys., 8, 5551-5563, doi:10.5194/acp-8-5551-2008, 2008.

Sirois, A., and Bottenheim, J.W.: Use of backward trajectories to interpret the 5-year record of PAN and O3 ambient air concentrations at Kejimkujik National Park, Nova Scotia, J. Geophys. Res., 100, 2867-2881, doi:10.1029/94JD02951, 1995.

Strickland, M.J., Darrow, L.A., Klein, M., Flanders, W.D., Sarnat, J.A., Waller, L.A., Sarnat, S.E., Mulholland, J.A., and Tolbert, P.E.: Short-term associations between ambient air pollutants and pediatric asthma emergency department visits, Am. J. Respir. Crit. Care Med., 182, 307-316, doi:10.1164/rccm.200908-1201OC, 2010.

Theodosi, C., Grivas, G., Zarmpas, P., Chaloulakou, A., and Mihalopoulos, N.: Mass and chemical composition of size-segregated aerosols (PM1, PM2.5, PM10) over Athens, Greece: local versus regional sources, Atmos. Chem. Phys., 11, 11895-11911, doi:10.5194/acp-11-11895-2011, 2011.

Tombrou, M., Dandou, A., Helmis, C., Akylas, E., Angelopoulos, G., Flocas, H., Assimakopoulos, V. and Soulakellis, N.: Model evaluation of the atmospheric boundary layer and mixed-layer evolution, Boundary-layer meteorology, *124*(1), 61-79, doi:10.1007/s10546-006-9146-5, 2007.

Turpin, B.J., and Huntzicker, J.J.: Identification of secondary organic aerosol episodes and quantification of primary and secondary organic aerosol concentrations during SCAQS, Atmos Environ, 29, 3527–3544, doi: 10.1016/1352-2310(94)00276-Q, 1995.

Ulbrich, I. M., Canagaratna, M. R., Zhang, Q., Worsnop, D. R., and Jimenez, J. L.: Interpretation
  of organic components from Positive Matrix Factorization of aerosol mass spectrometric data,
  Atmos. Chem. Phys., 9, 2891-2918, doi:10.5194/acp-9-2891-2009, 2009.

Ulbrich, I.M., Handschy, A., Lechner, M., and Jimenez, J.L. AMS Spectral Database. URL:
  http://cires.colorado.edu/jimenez-group/AMSsd/, Database Version 5.2, Last Updated 2013.

Wang, Y.Q., Zhang, X.Y., Draxler, R.: TrajStat: GIS-based software that uses various trajectory
  statistical analysis methods to identify potential sources from long-term air pollution
  measurement data, Environ. Mod. Softw., 24, 938–939, doi:10.1016/j.envsoft.2009.01.004,
  2009.

Wilhelm, M., Ghosh, J.K., Su, J., Cockburn, M., Jerrett, M., and Ritz, B.: Traffic-related air toxics
  and preterm birth: a population-based case-control study in Los Angeles county, California,
  Environ. Health, 10, 89, doi:10.1186/1476-069X-10-89, 2011.

Zanobetti, A., Franklin, M., Koutrakis, P., and Schwartz, J.: ine particulate air pollution and its
  components in association with cause-specific emergency admissions, Environ. Health Global
  Access. Sci., 8, 58, doi:10.1186/1476-069X-8-58, 2009.
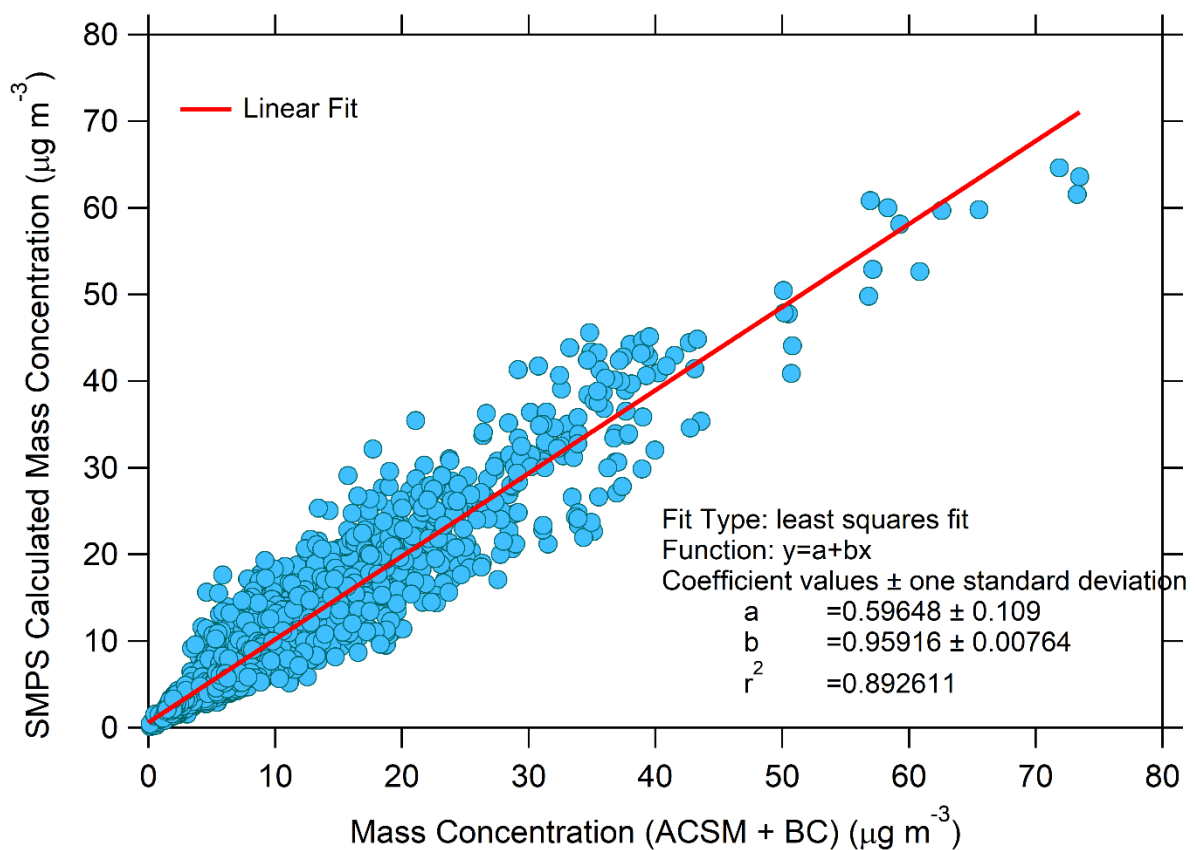
Figure 1: Correlation between ACSM+BC vs. SMPS-derived 1 – hour averaged mass concentrations for the 2016-17 measurement period.

1005
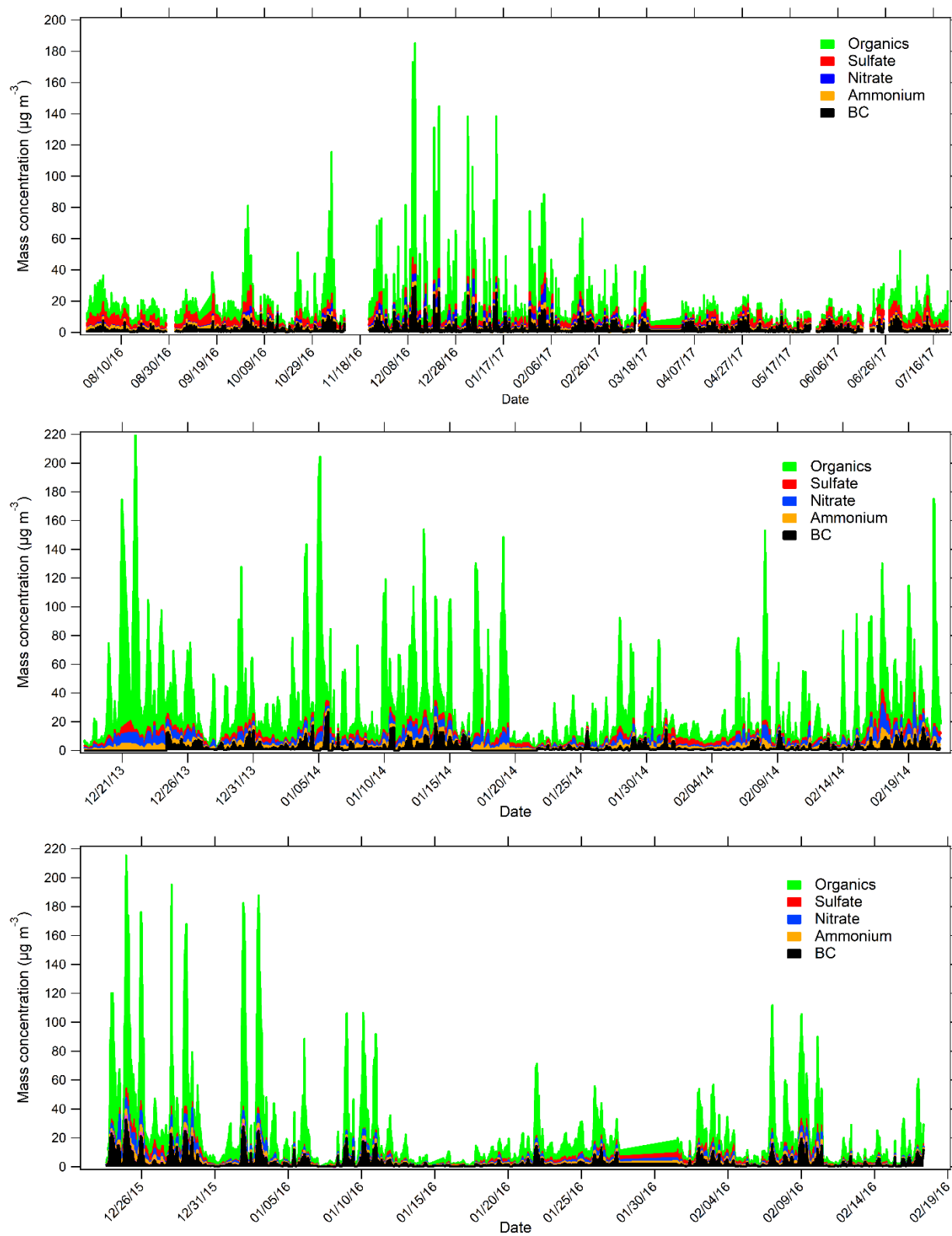
Figure 2: Time series of the main submicron aerosol components. On the top panel the one-year period starting on 26 July 2016 and ending on 31 July 2017, on the middle panel the 2013-2014 winter campaign

1010   (18 December-21 February), and on the bottom panel, the 2015-2016 winter campaign (23 December-17

February).
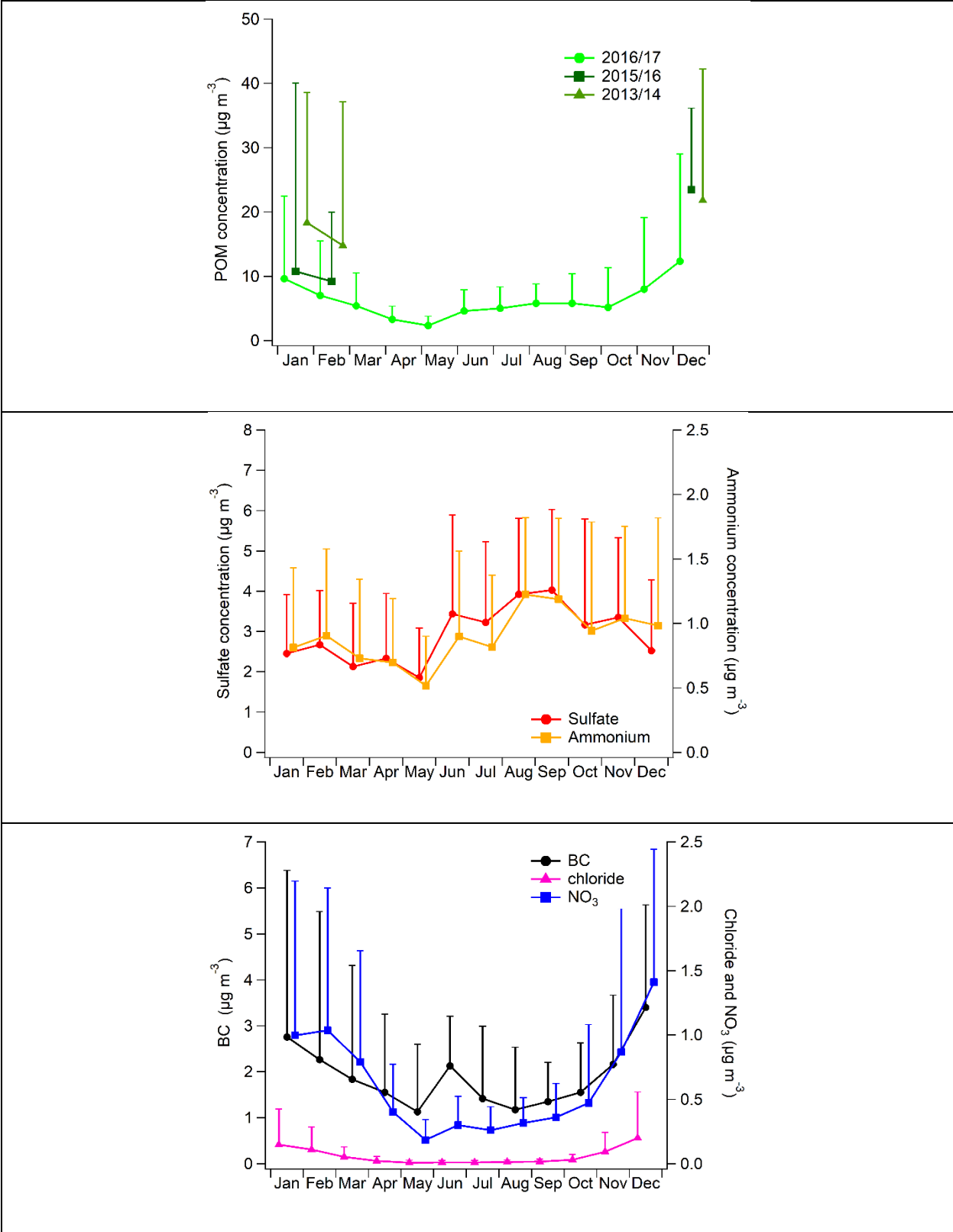
Figure 3: Monthly average concentrations of the main aerosol constituents. Organics are shown on the top panel for the one year 2016-2017 period as well as the 2013-2014 and 2015-2016 winter periods, while

 sulfate and ammonium on the middle panel, and BC, nitrate and chloride on the bottom panel shown for the one year 2016-2017 period. Standard deviation is also depicted (error bars; only the positive part is shown for plot's clarity issues).

1020
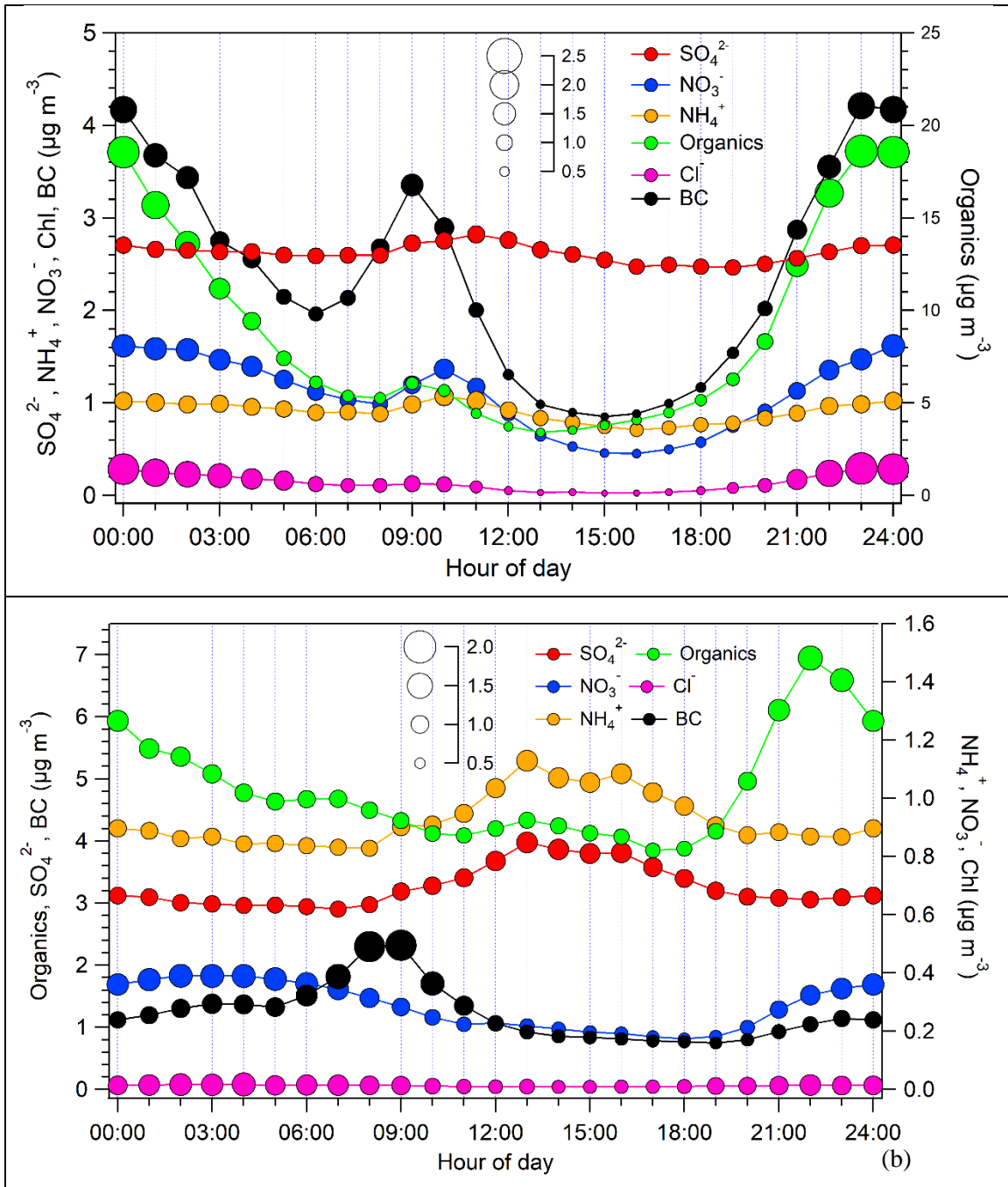
Figure 4: Average daily cycle of the main submicron aerosol constituents for the cold period 2016-17 on the top panel and the warm period of 2017 on the bottom panel. The size of the markers indicates the normalized values relative to each species' daily mean value.
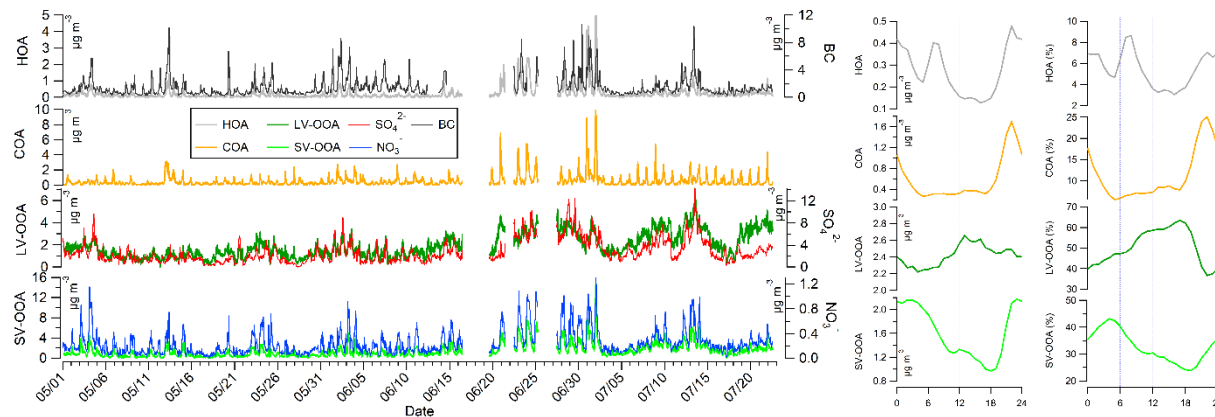
Figure 5: Time series of the contribution of the different factors identified by PMF between 1 May – 31 July 2017 (left) along with their average diurnal cycles (middle) and the respective hourly average contributions (right).
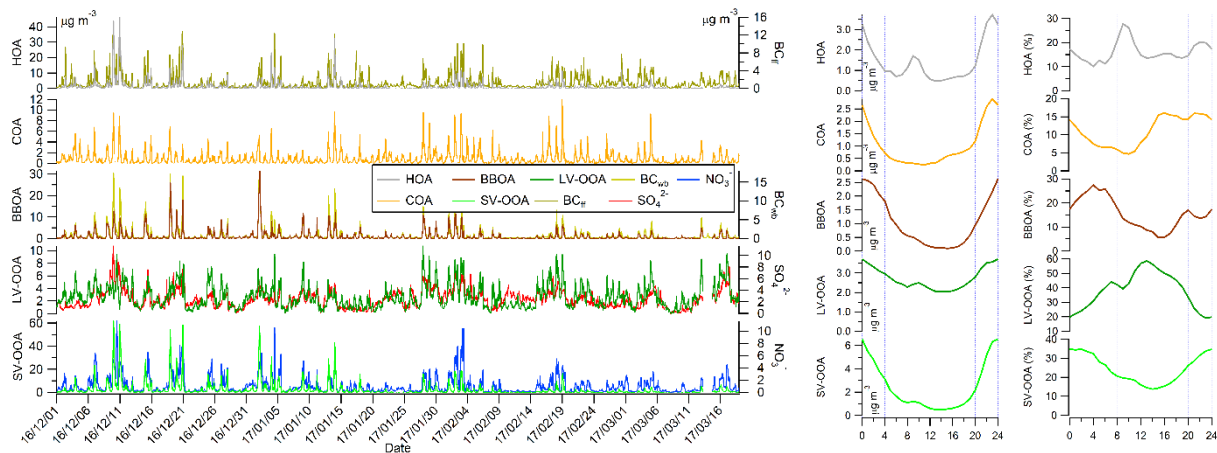
1035 **Figure 6:** Time series of the contribution of the different factors identified by PMF between 21 Nov. 2016 – 1 March 2017 (left) along with their average diurnal cycle (middle) and respective hourly contribution (right).
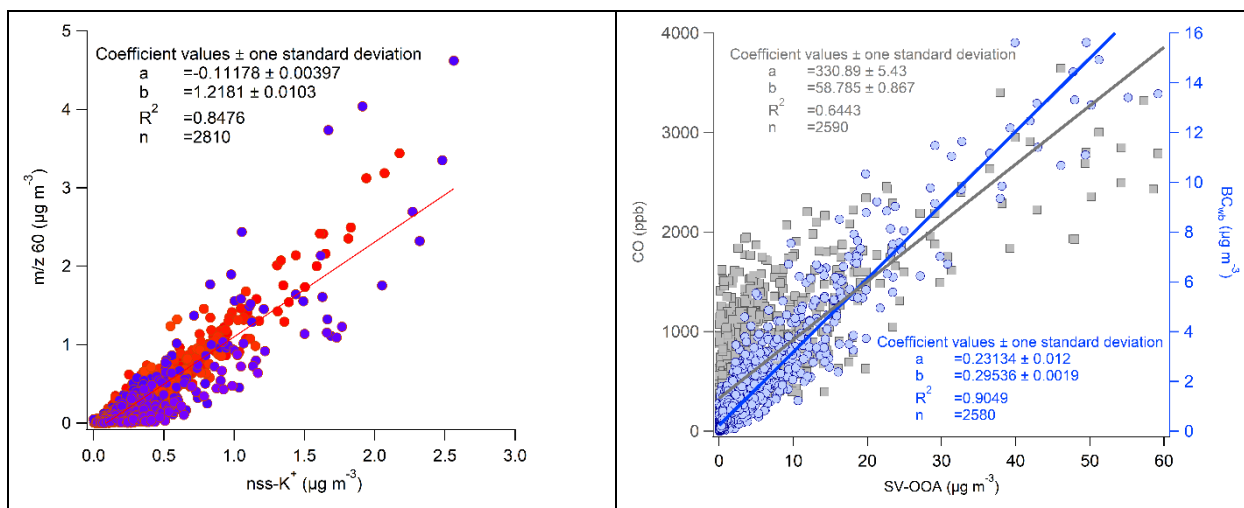
Figure 7: (a) Correlation of m/z 60 with nss-K$^+$ for 2013-14 (red) and 2016-17 (blue), and (b) Correlation of SV-OOA with CO (grey) and BC (blue) for 2016-17.

1040

	Mar – Apr – May 2017	Jul-Aug 2016 & Jun- Jul 2017	Sep – Oct – Nov 2016	Dec – Jan – Feb 2016-2017	Dec – Jan – Feb 2013-2014	Dec – Jan – Feb 2015-2016
			(a)			(b)

Organics	3.3 ± 3.0 (0.3-31.3)	5.4 ± 3.4 (0.3-41.9)	6.1 ± 7.5 (0.1-98.2)	9.0 ± 13.4 (0.2-153.9)	18 ± 24.4 (0.4-212.2)	12.4 ± 19.9 (0.7-1150.5)
Ammonium	0.6 ± 0.5 (0.4-3.1)	1.0 ± 0.6 (0.2-4.1)	1.0 ± 0.7 (0.4-5.7)	0.9 ± 0.7 (0.2-5.7)	1.8 ± 1.2 (0.2-9.1)	1.1 ± 1 (0.3-6.7)
Sulfate	2.1 ± 1.5 (0.2-10.1)	3.6 ± 2.1 (0.3-14.9)	3.5 ± 2.3 (0.1-17.1)	2.5 ± 1.5 (0.1-11.7)	2.6 ± 1.4 (0.4-13.9)	2.2 ± 1.7 (0.4-10.3)
Nitrate	0.4 ± 0.5 (0.05-5.4)	0.3 ± 0.2 (0.01-1.5)	0.5 ± 0.7 (0.1-6.9)	1.2 ± 1.5 (0.05-12.1)	2.6 ± 2.4 (0.09-18.3)	1.5 ± 1.4 (0.07-16)
Chloride	0.02 ± 0.05 (0-0.8)	0.02 ± 0.02 (0.04-0.2)	0.04 ± 0.09 (0.07-2.0)	0.15 ± 0.3 (0-3.5)	0.16 ± 0.24 (0.09-8.1)	0.12 ± 0.24 (0-2.6)
BC	1.5 ± 1.4 (0.1-14.6)	1.2 ± 0.8 (0.2-10.5)	1.7 ± 1.6 (0.1-12.4)	2.4 ± 3.4 (0.1-29.6)	2.7 ± 3.2 (0.2-26.8)	3.4 ± 4.6 (0.2-32.3)
PM1	8.9 ± 6.1 (0.6-42.4)	10.3 ± 5.6 (0.5-52.2)	13 ± 11.1 (0.9-115.5)	16.1 ± 19.5 (0.8-185.8)	24.5 ± 24.7(1.4-227.2)	21.2 ± 27.4 (1.7-215.3)

Table 1: Seasonal average concentrations ± standard deviation (range) and total mass of the main submicron aerosol components for the one-year study period and the two winter campaigns.

	Winter 2013-14 18/12/13 – 21/02/14	Winter 2015-16 23/12/15 – 17/02/16	Cold 2016-17 01/11/16-18/03/17
BBOA	12.4%	8.9%	11.9%
HOA	12.2%	9.7%	16.4%
COA	10.4%	8.1%	11.7%
SV-OOA	19.8%	17.7%	28%
LV-OOA	45.2%	55.6%	32%

Table 2: Contribution of the five organic aerosol components to the total organic fraction during the three individual winter campaigns.